ฟังชันนัลความหนาแน่นของการเปลี่ยน 2,3-ไดเมทิล-2,3-บิวเทนไดอัล และ
2,3-ไดเมทิล-2,3-เพนเทนไดอัล ในระบบเร่งปฏิกิริยาด้วยกรด

นายทัศน์ทนุ ฌานยิบ

วิทยานิพนธ์นี้เป็นส่วนหนึ่งของการศึกษาตามหลักสูตรปริญญาวิทยาศาสตรมหาบัณฑิต
สาขาวิชาปิโตรเคมีและวิทยาศาสตร์พอลิเมอร์
คณะวิทยาศาสตร์ จุฬาลงกรณ์มหาวิทยาลัย
ปีการศึกษา 2549

DENSITY FUNCTIONAL STUDY OF CONVERSIONS OF 2,3-DIMETHYL-2,3-BUTANEDIOL AND 2,3-DIMETHYL-2,3-PENTANEDIOL IN ACID-CATALYZED SYSTEMS

Mr. Tadtanu Shanyib

A Thesis Submitted in Partial Fulfillment of the Requirements
for the Degree of Master of Science program in Petrochemical and Polymer Science
Faculty of Science
Chulalongkorn University
Academic Year 2006

Thesis title	DENSITY FUNCTIONAL STUDY OF CONVERSIONS OF 2,3-DIMETHYL-2,3-BUTANEDIOL AND 2,3-DIMETHYL-2,3-PENTANEDIOL IN ACID-CATALYZED SYSTEMS
By	Mr. Tadtanu Shanyib
Field of study	Petrochemistry and Polymer Science
Thesis Advisor	Associate Professor Vithaya Ruangpornvisuti, Dr.rer.nat.

Accepted by the Faculty of Science, Chulalongkorn University in Partial Fulfillment of the Requirements for the Master's Degree

..................................Dean of the Faculty of Science
(Professor Piamsak Menasveta, Ph.D.)

Thesis committee

..................................Chairman
(Professor Pattarapan Prasassarakich, Ph.D.)

..................................Thesis Advisor
(Associate Professor Vithaya Ruangpornvisuti, Dr.rer.nat.)

W. Trakarnpruk ....Member
(Associate Professor Wimonrat Trakarnpruk, Ph.D.)

..................................Member
(Associate Professor Buncha Pulpoka, Ph.D.)

ทัศน์ทนุ ฌานยิบ : ฟังก์ชันนัลความหนาแน่นของการเปลี่ยน 2,3-ไดเมทิล-2,3-บิวเทนไดอัล และ 2,3-ไดเมทิล-2,3-เพนเทนไดอัล ในระบบเร่งปฏิกิริยาด้วยกรด (DENSITY FUNCTIONAL STUDY OF ONVERSIONS OF ,3-DIMETHYL-2,3-BUTANEDIOL AND 2,3-DIMETHYL-2,3-PENTANEDIOL IN ACID-CATALYZED SYSTEMS).อ.ที่ปรึกษา : รศ.ดร.วิทยา เรืองพรวิสุทธิ์; 73 หน้า

ศึกษาปฏิกิริยาการเปลี่ยนของสาร 2,3-ไดเมทิล-2,3-บิวเทนไดอัล ไปเป็น 2,3-ไดเมทิล-1,3-บิวทาไดอีน และ 2,3-ไดเมทิล-2,3-เพนเทนไดอัล ไปเป็น 2,3-ไดเมทิล-1,3-เพนทาไดอีน โดยใช้ระบบที่มีกรดเป็นตัวเร่งปฏิกิริยา ด้วยวิธีการคำนวณทางทฤษฎีฟังก์ชันนัลความหนาแน่นที่ระดับการคำนวณทางควอนตัม B3LYP/6-31G(d) และ B3LYP/6-311+G(d,p) ค่าพลังงานทางเทอร์โมไดนามิกและพลังงานของทุกขั้นในปฏิกิริยาสามารถได้จากการทดลอง ผลจากการศึกษาพบว่าค่าพลังงานกระตุ้นของปฏิกิริยาการเปลี่ยน 2,3-ไดเมทิล-2,3-บิวเทนไดอัล และเมื่อมีการเติมโมเลกุลน้ำเข้าสู่ปฏิกิริยาการเปลี่ยน 2,3-ไดเมทิล-2,3-บิวเทนไดอัล เมื่อมีกรดเป็นตัวเร่งปฏิกิริยามีค่า 55.13(60.17) และ 26.21(30.42) กิโลแคลอรีต่อโมลตามลำดับ และค่าพลังงานกระตุ้นของปฏิกิริยาการเปลี่ยน 2,3-ไดเมทิล-2,3-เพนเทนไดอัล และเมื่อมีการเติมโมเลกุลน้ำเข้าสู่ปฏิกิริยาการเปลี่ยน 2,3-ไดเมทิล-2,3-เพนเทนไดอัล เมื่อมีกรดเป็นตัวเร่งปฏิกิริยามีค่า 69.74(67.15) และ 20.12(29.05) กิโลแคลอรีต่อโมลตามลำดับ (ค่าในวงเล็บคือค่าที่ได้จากวิธี B3LYP/6-31G(d)) แสดงให้เห็นว่าค่าพลังงานกระตุ้นของปฏิกิริยาของสารตั้งต้นทั้งสองชนิด จะลดลงเมื่อมีการเติมโมเลกุลน้ำเข้าสู่ปฏิกิริยา เนื่องจากโมเลกุลน้ำมีความสามารถคล้ายเบสในปฏิกิริยา จึงช่วยในการดึงโปรตอนออกจากตัวกลางในปฏิกิริยาได้

สาขาวิชา ปิโตรเคมีและวิทยาศาสตร์พอลิเมอร์ ลายมือชื่อนิสิต ทัศน์ทนุ ฌานยิบ

ปีการศึกษา 2549 ลายมือชื่ออาจารย์ที่ปรึกษา

4672269023: PETROCHEMISTRY AND POLYMER SCIENCE.
KEYWORD: PINACOL REARRANGEMENT; DFT

TADTANU SHANYIB: DENSITY FUNCTIONAL STUDY OF CONVERSIONS OF 2,3-DIMETHYL-2,3-BUTANEDIOL AND 2,3-DIMETHYL-2,3-PENTANEDIOL IN ACID-CATALYZED SYSTEMS
THESIS ADVISOR: ASSOC. PROF. VITHAYA RUANGPORNVISUTI, Dr.rer.nat.73 pp.

Conversion reactions of 2,3-dimethyl-2,3-butanediol (DMBDOL) to 2,3-dimethyl-1,3-butadiene (DMBDENE) and 2,3-dimethyl-2,3-pentanediol (DMPDOL) to 2,3-dimethyl-1,3-pentadiene (DMPDENE) in acid-catalyzed system have been investigated using density functional theory method at B3LYP/6-31G(d) and B3LYP/6-311+G(d,p) levels of theory. Activation energies of conversion reaction of 2,3-dimethyl-2,3-butanediol (DMBDOL) and 2,3-dimethyl-2,3-butanediol with molecule of water in acid-catalyzed systems are 55.13(60.17) and 26.21(30.42) kcal/mol, respectively. The activation energy of conversion reaction of 2,3-dimethyl-2,3-pentanediol (DMPDOL) and 2,3-dimethyl-2,3-pentanediol with molecule of water in acid-catalyzed systems is 69.74(67.15) and 20.12(29.05) kcal/mol, respectively (method B3LYP/6-31G(d) is in the parenthesis). The activation energy of the conversion reaction of 2,3-dimethyl-2,3-butanediol and 2,3-dimethyl-2,3-pentanediol are decreased when the water molecule was added. The water molecule is sufficient to affect protonation, can acts as a base to remove the adjacent protons from intermediates.

Field of study Petrochemistry and Polymer Science Student's signature ....
Academic year 2006 Advisor's signature ....

ACKNOWLEDGEMENTS

I would like to express my sincerest gratitude to my advisor, Associate Professor Dr.Vithaya Ruangpornvisuti, for all substantial advices, precious assistances, kind suggestions and encouragement throughout the course of this research.

The greatest thanks are extended to Professor. Dr. Pattarapan Prasassarakich, Associate Professor Dr. Wimonrat Trakarnpruk and Associate Professor Dr. Buncha Pulpoka for their suggestions and comments as the thesis committee. Moreover, I greatly appreciated the Petrochemistry and Polymer Science Program and Graduate School Chulalongkorn University for research grant.

Special thanks to all members in Supramolecular Chemistry Research Unit, Department of Chemistry, Faculty of Science, Chulalongkorn University, Bangkok, Thailand for their kind, friendship, support an for their worthy comments, valuable suggestions and encouragement. I also would like to thank all my friends at Chulalongkorn University for their friendship throughout my study.

Finally, I would like to affectionately give all my gratitude to my parents and all the members of my family for their love, understanding, encouragement and support throughout my entire study. Without them, I would never be able to achieve this goal.

CONTENTS

Page

LIST OF TABLES

LIST OF FIGURES

Figure **Page**

Figure **Page**

CHAPTER I

INTRODUCTION

1.1 Pinacol Rearrangement Mechanism

The pinacol rearrangement was the first molecular rearrangement identified as such by early chemists.*[1-3]* The defining example of a pinacol rearrangement is shown in Figure 1.1. Pinacol itself is produced by magnesium reduction of acetone, probably by way of a ketyl intermediate. Since the diol is symmetrical, protonation and loss of water takes place with equal probability at either hydroxyl group. The resulting 3º-carbocation is relatively stable, and has been shown to return to pinacol by reaction in the presence of isotopically labeled water. A 1,2-methyl shift generates an even more stable carbocation in which the charge is delocalized by heteroatom resonance. Indeed, this new cation is simply the conjugate acid of the ketone pinacolone, which is the product of repeated rearrangements catalyzed by proton transfer. Each step in this rearrangement is potentially reversible, as demonstrated by the acid catalyzed dehydration of pinacolone (and pinacol) to 2,3-dimethyl-1,3-butadiene under vigorous conditions.

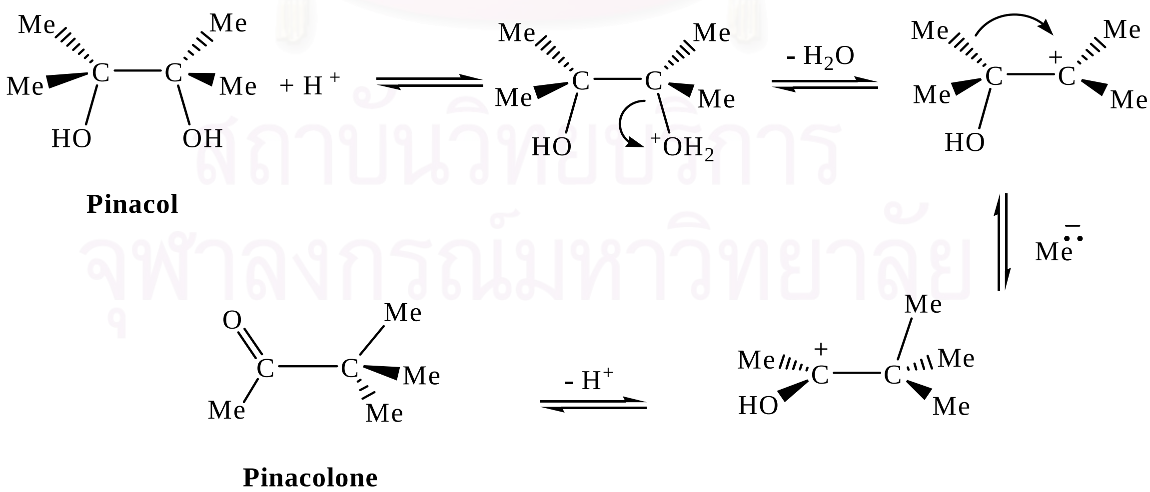

Figure 1.1 Pinacol rearrangement of pinacol to pinacolone.

There are two possible reaction pathways for the pinacol rearrangement. One is the stepwise mechanism *via* a carbonium ion intermediate, and the other is the concerted mechanism where migration and elimination occur simultaneously, as shown in Figure 1.2.

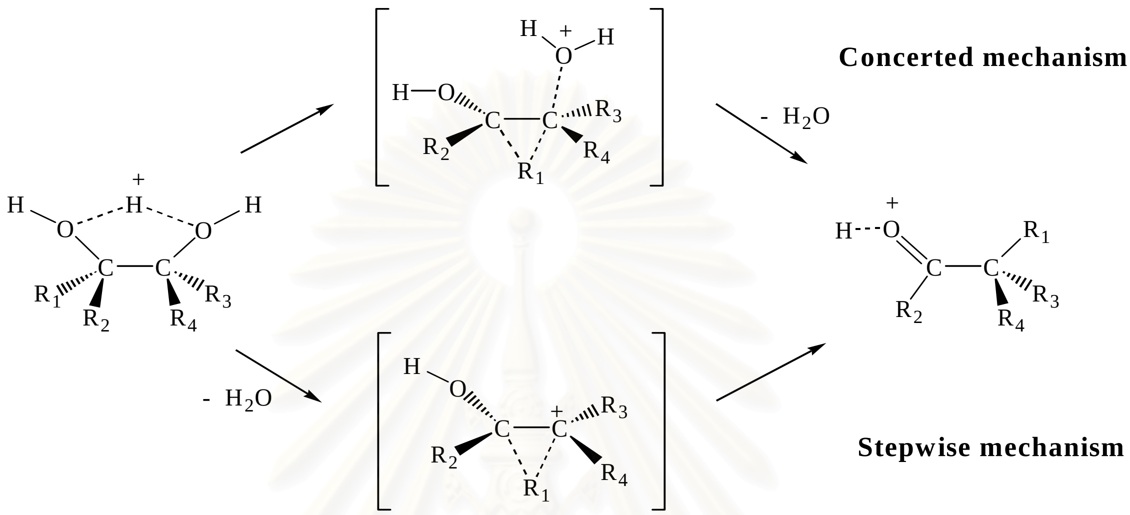

Figure 1.2 Pinacol rearrangement mechanism and 1, 2-elimination mechanism.

The rearrangements of many reactions involve not only the stepwise but also the concerted mechanism. Nakamura and Osamura *[4-5]*, who studied the reaction mechanism and migratory aptitude of the pinacol rearrangement in the gas-phase calculation, stated that overall activation energy for the stepwise mechanism was higher than that of the concerted mechanism. This signifies that concerted mechanism is more favorable mechanism. Their results were in good agreement with experimental results for pinacol reactions in gas-phase and nonpolar solution. The effect of various acids at different concentrations on the pinacol rearrangement was investigated by Lezaeta *et al. [6]*. They reported that the pinacolone was the principle product and its relative yield decreased when the acid concentration was lowered. The pinacol rearrangement process was also carried out using different acid catalysts such as silica-alumina, zeolite, silicoaluminophosphates and perfluorinate resinsulfonic acids *[7-9]*.

The pinacol rearrangement of asymmetric diol is given more than one product because each protonated hydroxyl group is not identical. For example, when propylene glycol is protonated, two possible geometries of protonated propylene glycol are found. The first geometry generates the primary carbocation and the other geometry generates the secondary carbocation, as shown in Figure 1.3.

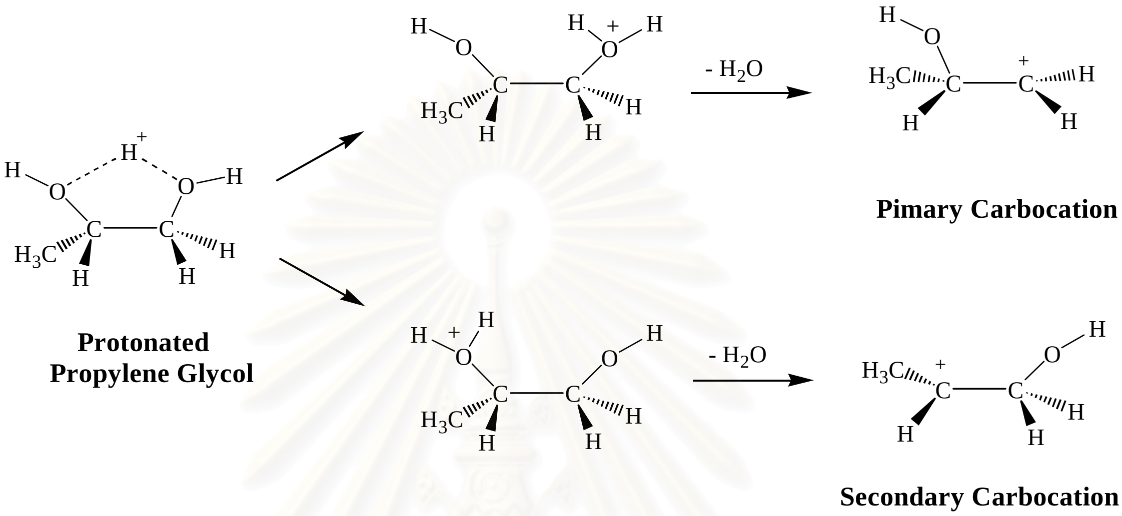

Figure 1.3 Dehydration pathways of protonated propylene glycol.

The dehydration is favored on the substituted carbon because the produced carbocation is stabilized by electron delocalization from the substitute group. The pinacol rearrangements of asymmetric diol have been studied in several conditions such as sulfuric acid, $AlCl_3$ and heteropoly acid *[10-12]*.

Many works of rearrangement reactions have been investigated by theoretical study.*[13-18]* A theoretical study of the mechanism both stepwise and concerted reactions has been described by Nakamura and Osawara aboved. Although, a major product of pinacol rearrangement is the pinacolone, but the 2,3-dimethyl-1,3-butadiene becomes the major product by some cases.*[19]* The pinacol rearrangement reaction with increasing dilution of the acid by water or conjugate base, the mechanistic pathway is shifted toward elimination*[20]*. Because of the increasing amount of water, which can act as a base to remove the adjacent protons from intermediates to afford 2,3-dimethyl-1,3-butadiene, as shown in Figure 1.4. The classical rearrangement leading to pinacolone (1) proceeds *via* protonation of the hydroxyl group and subsequent loss of water to afford the stable carbocation (A), which undergoes a 1,2-shift to form the more stable intermediate (B). Alternatively, (A) can lose a proton to form 2,3-dimethyl-3-butene-2-ol (3). Protonation of the hydroxyl group in 2,3-dimethyl-3-butene-2-ol and loss of water leads to allylic carbocation (C) that yields 2,3-dimethyl-1,3-butadiene (2) as the main elimination product. Addition products, 1-halo-2,3-dimethyl-2-butene (4) and 3-halo-2,3-dimethyl-1-butene (5), were also observed when a hydrogen halide (HX = HCl or HBr) was used as the catalyst. By virtue of resonance structure (C), reduction product (6) was also obtained when HI served as the acid.

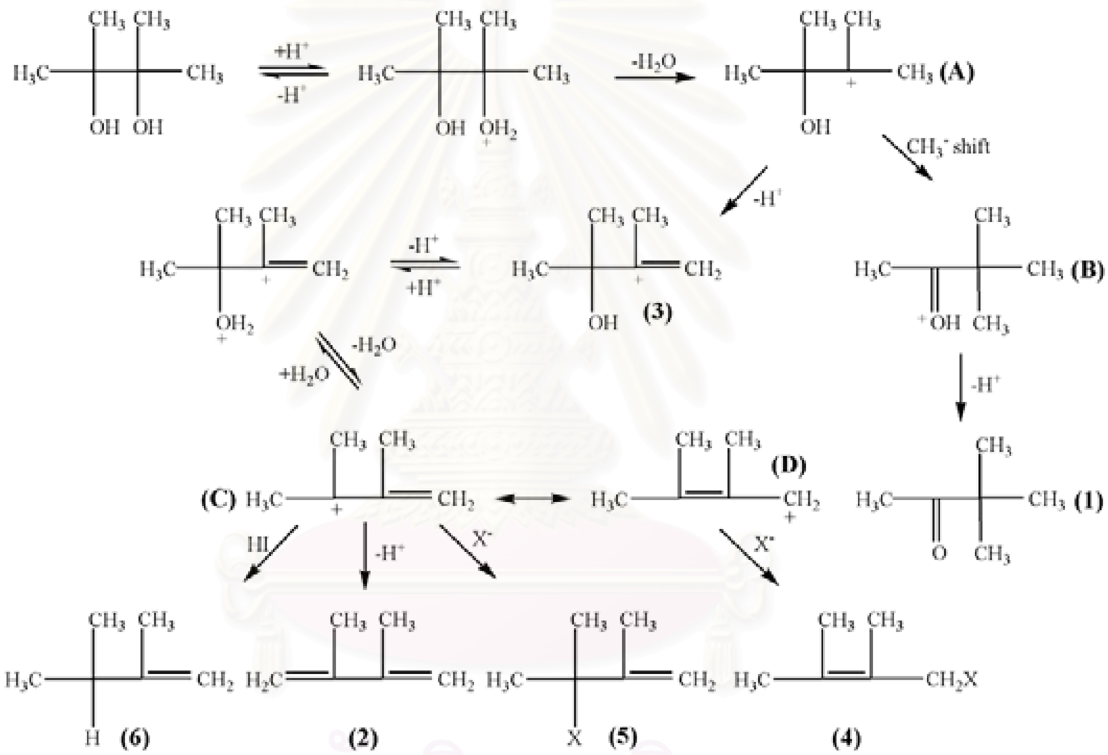

Figure 1.4 The rearrangement pathways of pinacol (2,3-dimethy-2,3-butanediol) to pinacolone and alternative routh leading to another products.*[20]*

Hsu and Cheng (1998) *[21]* found that pinacol rearrangement proceeds at relatively mild temperature over metal-substituted aluminophosphate molecular sieves. The conversion of pinacol and the selectivity of the product were found to influenced by the metal species. Fe(III), Cu(II) and Ni(II) are the three which gave the highest pinacol conversion and pinacolone selectivity. The catalytic activity was found to have no direct correlation with the acid strength and amount of the acid site on the catalysts. The mechanism involving the redox ability of Fe(III) and its stabilization of the carbonium ion intermediates are proposed. Kita *et al.* (1997) *[22-23]* reported an efficient pinacol rearrangement by trialkyl orthoformate. The reactions of various types of diols with a catalytic amount of a Lewis acid in the presence of an ortho ester afforded the rearranged product in good yields via a cyclic ortho ester intermediate. The combined system was applicable not only to cyclic and acyclic tri- and tetra-substituted diols but also to the diols having acid-sensitive acetals. Ikushima *et al.* (2000) *[24]* studied on pinacol rearrangement using supercritical water (scH_2O) by a high-pressure and high-temperature (FTIR). They found that significant acceleration of pinacol rearrangement can be achieved by using supercritical water, especially near the critical point, even in the absence of any acid catalysts. The rate of pinacol rearrangement using supercritical water is significantly larger by a factor of 28,200 than that in 0.871 M HCl solution at 46.7 MPa under distillation conditions. The activation energy for the former at 25 MPa was found to be markedly reduce to about one-third of that for the latter. The accelerated rates of reaction may be attributed to a great increase in the local proton concentration around the organic reactants.Cheng *et al.* (2002) *[25]* studied on pinacol-type rearrangement reactions in toluene which were catalyzed by iron-substituted molecular sieves of different porous structures, including AlPO4-5, ZSM-5 of micropores and MCM-41 of mesopores. Iron(III)-substitute in the framework of the molecular sieves was found to be the active center for pinacol rearrangement reaction and catalytic activity was found to have no correlation with the acidity. Ten vicinal diol reactants with various alkyl or aryl substitutions were examined. The migrating preference of the substitution groups was dependent on the catalysts and the migration attitude was different from that observed on acid-catalyzed reactions. Smith (2002) *[26]* proposed two possible mechanisms for rearrangement of ethylene glycol to acetaldehyde. Density functional theory at the 6-31G(d) level had been applied to answer the question of whether the pinacol rearrangement of ethylene glycol proceeds through a dehydration to enol the forming acetaldehyde or by a concerted migration of hydride with loss of water. The result was shown that the latter process had activation energy lower than the route through the enol intermediate. Dai *et al.* (2004) *[27]* carried out the dehydration of propylene glycol in near-critical water to study the reactivity of diol under high temperature and pressure. The investigation of reaction mechanism indicated that there were two mechanisms, pinacol rearrangement and elimination mechanisms, to be possible in the dehydration of propylene glycol. Pachuau *et al.* (2004) *[28]* used the semi- empirical PM3 SCF-MO method to investigate the Wagner–Meerwein migration of various groups during the pinacol-pinacolone rearrangement of some acyclic systems. The 1,2-migration was found to involve a three-centered moiety in the cationic transition state. The structures of the migratory groups in the transition state and migratory aptitude were reported. Ruangpornvisuti and rungnim (2004) *[29]* used the density functional method at 298.15 K to investigate the acid-catalyzed model on reaction mechanisms of pinacol rearrangement of propylene glycol conversion to propanol and propanone. Thermodynamic quantities of activation steps of water addition models were obtained. They found that, the percent ratios of propanal and propanone were decreased as the amount of added water increased.

1.2 Overall Objectives

The aim of this study is to investigate conversion mechanism of 2,3-dimethyl-2,3-butanediol (DMBDOL) to 2,3-dimethyl-1,3-butadiene (DMBDENE) and 2,3-dimethyl-2,3-pentanediol (DMPDOL) to 2,3-dimethyl-1,3-pentadiene (DMPDENE) in acid-catalyst system using density functional theory at B3LYP/6-31G(d) and B3LYP/6-311+G(d,p) level of theory. The energetic barriers and thermodynamic quantities of all related reactions have been computed at the same level of theory. All mechanisms of conversion reaction of 2,3-dimethyl-2,3-butanediol (DMBDOL) to 2,3-dimethyl-1,3-butadiene (DMBDENE) and 2,3-dimethyl-2,3-pentanediol (DMPDOL) to 2,3-dimethyl-1,3-pentadiene (DMPDENE) in acid catalyzed systems have been proposed.

CHAPTER II

THEORY

Computational chemistry is a set of techniques for investigating chemical problems on a computer.*[30]* The computational chemistry is concerned with the calculating and predicting the properties of atomic and molecular systems. It is based on the fundamental laws of quantum mechanics and uses a variety of mathematical transformation and approximation techniques to solve the fundamental equations. This section provides an introduction overview of the theory underlying electronic structure methods.

2.1. Quantum Mechanics

Quantum mechanics (QM) is the mathematical description of the behavior of electrons and thus of chemistry.*[31]* In theory, QM can predict any property of an individual atom or molecule exactly. In practice, the QM equations have only been solved exactly for one electron systems. A myriad collection of methods has been developed for approximating the solution for multiple electron systems. These approximations can be very useful, but this requires an amount of sophistication on the part of the researcher to know when each approximation is valid and how accurate the results are likely to be.

Two equivalent formulations of QM were devised by Schrödinger and Heisenburg. However, the uncertainty principle of Heisenburg, which is authentically the limitation of the obtained microscopic information of a system, seems to be essential as the consequences of the wave-particle duality. Here, only the Schrödinger form, since it is the basis for nearly all computational chemistry methods, has been briefly reviewed.

The Schrödinger equation is

$$\hat{H}\Psi = E\Psi \tag{2.1}$$

where $\hat{H}$ is the Hamiltonian operator, Ψ the wavefunction, and E the energy. In the language of mathematics, an equation of this form is called and eigen equation. Ψ is then called the eigenfunction and E an eigenvalue. The operator and eigenfunction can be a matrix and vector, respectively, but this is not always the case.

The wave function Ψ is a function of the electron and nuclear positions. As the name implies, this is the description of an electron as a wave. This is a probabilistic description of electron behavior. As such, it can describe the probability of electrons being in certain locations, but it cannot predict exactly where electrons are located. The wavefunction is also called a probability amplitude because it is the square of the wavefunction that yields probabilities. This is the only rigorously correct meaning of a wavefunction. In order to obtain a physically relevant solution of the Schrödinger equation, the wavefunction must be continuous, single-valued, normalizable, and antisymmetric with respect to the interchange of electrons.

For molecule, the Hamiltonian operator $\hat{H}$ is, in general,

$$\hat{H} = \hat{T} + \hat{V} \tag{2.2}$$

where for a molecule,

$$\hat{T} = \hat{T}_n + \hat{T}_e = -\sum_{A=1}^{N} \frac{1}{2M_A}\nabla^2{}_A - \sum \frac{1}{2}\nabla_i^2 \tag{2.3}$$

where $\nabla^2{}_A$ and $\nabla^2{}_i$ are the Laplacian operators acted on nuclei and electrons, respectively.

$$\hat{V} = \hat{V}_{ne} + \hat{V}_{ee} + \hat{V}_{nn} = -\sum_{i=1}^{n}\sum_{A=1}^{N} \frac{Z}{r_{iA}} + \sum_{i=1}^{n}\sum_{j<1}^{n} \frac{1}{r_{ij}} + \sum_{A=1}^{N}\sum_{B<A}^{N} \frac{Z_A Z_B}{R_{AB}} \tag{2.4}$$

From (2.3) to (2.4), the molecular Hamiltonian is,

$$\hat{H} = -\sum \frac{1}{2}\nabla_i^2 - \sum_{A=1}^{N} \frac{1}{2M_A}\nabla^2{}_A - \sum_{i=1}^{n}\sum_{A=1}^{N} \frac{Z}{r_{iA}} + \sum_{i=1}^{n}\sum_{j<1}^{n} \frac{1}{r_{ij}} + \sum_{A=1}^{N}\sum_{B<A}^{N} \frac{Z_A Z_B}{R_{AB}} \tag{2.5}$$

in which A and B referred to nuclei and i and j referred to electrons. The first and second terms in equation 2.5 are the operators for the kinetic energy of the electrons and nuclei, respectively. The third term is the electron-nuclear attraction where r_{iA} is the distance between electron i and nucleus A. The fourth term is the electron-electron repulsion where r_{ij} is the distance between electron i and j. The last term is the nuclear-nuclear repulsion where R_{AB} is the distance between nuclei A and B with atomic number Z_A and Z_B, respectively. This formation is time-independent. Additional terms can appear in the Hamiltonian operator where relativity or interaction or fields are taken into account. Furthermore, small magnetic effects, for example, spin-orbit coupling, spin-spin interactions, etc., are also omitted in this Hamiltonian.

In summary, whenever the Hamiltonian does not depend on time, one can solve the time-independent Schrödinger equation first and then obtain the time-dependent equation when the energy E is known. In the case of molecular structure theory, it is a quite daunting task even to approximately solve the full Schrödinger equation because it is a partial differential equation depending on all of the coordinates of the electrons and nuclei in the molecule. For these reason, there are various approximations that one usually implements when attempts to study molecular structure using quantum mechanics.

2.2 Ab initio Methods

The term *ab initio* is Latin for "from the beginning". This name is given to computations that are derived directly from theoretical principles with no inclusion of experimental data. This is an approximate quantum mechanical calculation. The approximations made are usually mathematical approximations, such as using a simpler functional form for a function or finding an approximate solution to a differential equation.

All molecular wavefunctions are approximate; some are just more approximate than otheres. We can solve the Schrödinger equation exactly for the hydrogen atom but not even, despite what many textbooks say, for the hydrogen molecule ion, H_2^+.

2.3 Basis Sets

Individual electrons to one-electron function, termed *spin orbital*. These consist of a product of spatial functions, termed *molecular orbitals (MO)*, $\psi_1(x,y,z)$,

$\psi_2(x,y,z)$, $\psi_3(x,y,z)$, ..., and either α or β spin components. The spin orbitals are allowed complete freedom to spread throughout the molecule. Their exact forms are determined to minimize the total energy. In the simplest level of theory, a single assignment of electron to orbital is made by used ψ as atomic orbital wavefunction based on the Schrödinger equation for the hydrogen atom. This is not a suitable approach for molecular calculation. This problem can be solved by representing MO as linear combination of basis functions.

In practical calculation, the molecular orbitals $\psi 1$, $\psi 2$, ..., are further restricted to be linear combinations of a set of N known one-electron function $\phi_1(x,y,z)$, $\phi_2(x,y,z)$, ..., $\phi_N(x,y,z)$:

$$\psi_i = \sum_{\mu=1}^{N} c_{\mu i}\phi_{\mu} \tag{2.6}$$

The functions ϕ_1, ϕ_2, ..., ϕ_N, which are defined in the specification of the model, are known as one-electron basis function called basis function. The set of basis functions is called basis set. If the basis functions are the atomic orbitals for the atoms making up the molecule, function in equation 2.10 is often described as the *linear combination of atomic orbitals* (LCAO). There are two types of basis function which commonly used in the electronic structure calculations, *Slater type orbitals* (STO) and *Gaussian type orbitals* (GTO).

The Slater orbitals are primarily used for atomic and diatomic systems where high accuracy is required and semiempirical calculations where all three- and four-center integrals are neglected. The Slater type orbitals have the function form

$$b = Ae^{-\zeta r} r^{n^*-1} Y_{lm}(\theta,\phi) \tag{2.7}$$

where parameter *n** and ξ are chosen to make the larger part of the orbitals look like atomic Hartree-Fock orbitals. There are a lot like hydrogen orbitals, but without the complicated nodal structure.

The Gaussian type orbitals can be written in terms of polar or cartesian coordinates

$$g = x^a y^b z^c e^{-\alpha r^2} Y_{lm}(\theta,\phi) \tag{2.8}$$

in which *a*, *b*, and *c* are integers and α is a parameter that is usually fixed. Primitive Gaussian function is shown in equation 2.12. Normally, several of these Gaussian functions are summed to define more realistic atomic orbitals basis functions, as shown below.

$$b_{\mu} = \sum_{p} k_{\mu p} g_{p}. \tag{2.9}$$

The coefficients $k_{\mu p}$ in this expansion are chosen to make the basis functions look as much like Slater orbitals as possible. Slater functions are good approximation to atomic wavefunctions but required excessive computer time more than Gaussian functions, while single-Gaussian functions are a poor approximation to the nearly ideal description of an atomic wavefunction that Slater function provides. The solution to the problem of this poor functional behavior is to use several Gaussians to approximate a Slater function. In the simplest version of this basis, n Gaussian functions are superimposed with fixed coefficients to form one-Slater type orbital. Such a basis is denoted STO-nG, and n = 3, 4, …, etc.

The limit of quantum mechanics involves an infinite set of basis function. This is clearly impractical since the computational expanse of molecular orbital calculations is proportional to the power of the total number of basis functions. Therefore, ultimate choice of basis set size demands on a compromise between accuracy and efficiency. The classification of basis sets is given below.

2.3.1 Basis set effects

A basis set is the mathematical description of the orbitals with in a system which in turn combine to approximate the total electronic wave-function, used to perform the theoretical calculation. Larger basis set more accurately approximate the orbitals by imposing fewer restrictions on the locations of the electrons in space. In the true quantum mechanical picture, electrons have affinity probability of existing anywhere in space; this limit corresponds to the infinite basis set expansion.

Standard basis set for electronic structure calculations use linear combinations of GAUSSIAN functions to form the orbitals. GAUSSIAN program offers a wide range of predefined basis set, which may be classified by the number and types of basis functions that they contain. Basis sets assign a group of basis functions to each atom within a molecule to approximate is orbitals. These basis function themselves are composed of a linear of GAUSSIAN function; such basis functions are referred to as contracted functions, and the component GAUSSIAN functions are referred to as primitives. A basis function consisting of a single GAUSSIAN function is termed uncontracted.

2.3.2 Minimal basis sets

Minimal basis sets contain the minimum number of functions needed for each atom, as in these examples:

H: 1s

C: 1s, 2s, $2p_x$, $2p_y$, $2p_z$

Minimal basis sets use fixed-size atomic-type orbitals. The STO-3G basis set is a minimal basis set (although it is not the smallest possible basis set). It uses three GAUSSIAN primitives per basis function, which accounts for the “3G” in its name. “STO” stands for “Slater-type orbitals” and the STO-3G basis set approximates Slater orbitals with GAUSSIAN functions.

2.3.3 Split valence basis sets

The first way that a basis set can be made larger is to increase the number of basis functions per atom. Split valence basis sets, such as 6-31G, have two or more sizes of basis function for each valence orbital. For example, hydrogen and carbon are represented as:

H: 1s, 1s′

C: 1s, 2s, 2s′, $2p_x$, $2p_x'$, $2p_y$, $2p_y'$, $2p_z$, $2p_z'$

where the primed and unprimed orbitals differ in size.

The double zeta basis sets, such as the Dunning-Huzinage basis set, form all molecular orbitals from linear combinations of two sizes of functions for each atomic orbital. Similarly, triple split valence basis sets, like 6-311G, use three sizes of contracted functions for orbital-type.

In split valence basis sets, additional basis functions (one contracted Gaussian plus some primitive Gaussians) are allocated to each valence atomic orbital. The resultant linear combination allows the atomic orbitals to adjust independently for a given molecular environment. Split valence basis sets are characterized by the number of functions assigned to valence orbitals. ‘Double zeta’ basis sets use two basis functions to describe valence electrons, ‘triple zeta’ use three functions, and so forth. Basis sets developed Pople and coworkers are denoted by the number of Gaussian functions used to describe inner and outer shell electron. Thus ‘6-31G’ describes an inner shell atomic orbital with a contracted Gaussian composed of six primitive Gaussians, an inner valence shell with a contracted Gaussian composed of three primitives, and an outer valence shell with one primitive. Other split-valence sets include 3-21G, 4-31G, and 6-31G.

2.3.4 Split all Orbitals basis set (Double Zeta Basis Sets)

Double zeta basis set is a member of minimum basis set replaced by two functions. In this way both core and valence orbitals are scaled in size. For some heavier atoms, double zeta basis sets may have slightly less than double the number of minimum basis set orbitals. For example, some double zeta basis sets for the atoms Ga - Br have 7 rather than 8 *s* basis functions, and 5 rather than 6 *p* basis functions.

The term “*double zeta*” arises from the fact that the exponent in a STO is often referred by the Greek letter “*zeta*”. Since it takes two orbitals with different exponents, it is called “*double zeta*”. The minimum basis set is “*single zeta*”. The normal abbreviation for a double zeta basis set is DZ. It is also quite common to use split valence basis sets where the valence orbitals are spitted into three functions. Basis sets where this is done for all functions are called triple zeta functions and referred to as TZ, TZP, TZ2P etc.

2.3.5 Polarized basis sets

Polarization functions can be added to basis sets to allow for non-uniform displacement of charge away from atomic nuclei, thereby improving descriptions of chemical bonding. Polarisation functions describe orbitals of higher angular momentum quantum number than those required for the isolated atom (*e.g*., p-type functions for H and He, and d-type functions for atoms with Z > 2), and are added to the valence electron shells. For example, the 6-31G(d) basis set is constructed by adding six *d*-type Gaussian primitives to the 6-31G description of each non-hydrogen atom. The 6-31G(d,p) is identical to 6-31G(d) for heavy atoms but adds a set of Gaussian *p*-type functions to hydrogen and helium atoms. The additional of *p*-orbitals to hydrogen is particularly important in systems where hydrogen is a bridging atom. The polarization functions are added to the 6-31G basis set as follows:

6-31G* - added a set of d orbitals to the atoms in the first and second rows (Li-Cl).

6-31G** - added a set of d orbitals to the atoms in the first and second rows (Li-Cl) and a set of *p* functions to hydrogen.

The nomenclature above is slowly being replaced. The 6-31G* is called 6-31G(d), while the 6-31G** is called 6-31G(d,p). This new nomenclature allows the possibility of adding several polarization functions. Thus 6-31G(3df,pd) added 3 *d*-type GTOs and 1 *f*-type GTO to atoms Li-Cl and added 1 *p*-type and 1 *d*-type function to H.

2.3.6 Diffuse basis sets

Species with significant electron density far removed from the nuclear centers (e.g., anions, lone pairs and excited states) require diffuse functions to account for the outermost weakly bound electrons. Diffuse basis sets are recommended for calculations of electron affinities, proton affinities, inversion barriers and bond angles in anions. The addition of diffuse *s*- and *p*-type Gaussian functions to non-hydrogen atoms is denoted by a plus sign-as in ‘3-21+G’. Further addition of diffuse functions to both hydrogen and larger atoms is indicated by a double plus. The diffuse functions added to the 6-31G basis set as follows:

6-31+G - added a set of diffuse *s* and *p* orbitals to the atoms in the first and second rows (Li-Cl).

6-31++G - added a set of diffuse *s* and *p* orbitals to the atoms in the first and second rows (Li-Cl) and a set of diffuse *s* functions to hydrogen.

Diffuse functions can be added along with polarization functions also. Some examples of these functions are 6-31+G*, 6-31++G*, 6-31+G** and 6-31++G** basis sets.

2.4 Density Functional Theory

Density functional theory (DFT) has become very popular in recent years. This is justified based on the pragmatic observation that it is less computationally intensive than other methods with similar accuracy. This theory has been developed more recently than other *ab initio* methods. Because of this, there are classes of problems which are not yet explore with this theory, making it all the more crucial to test the accuracy of the method before applying it to unknown systems.

The premise behind DFT is that the energy of a molecule can be determined from the electron density instead of a wavefunction. This theory originated with a theorem by Hohenburg and Kohn that stated this was possible. The original theorem applied only to finding the ground-state electronic energy of a molecule. A practical application of this theory was developed by Kohn and Sham who formulated a method similar in structure to the Hartree-Fock method.

In this formulation, the electron density is expressed as a linear combination of basis functions similar in mathematical form to HF orbitals. A determinant is them formed from these functions, called Kohn-Sham orbitals. It is the electron density from this determinant of orbitals that is used to compute the energy. This procedure is necessary because Fermion systems can only have electron densities that arise from an antisymmetric wavefunction. There has been some debate over the interpretation of Kohn-Sham orbitals. It is certain that they are not mathematically equivalent to either HF orbitals or natural orbitals from correlated calculations. However, Kohn-Sham orbitals do describe the behavior of electrons in a molecule, just as the other orbitals mentioned do. DFT orbital eigenvalues do not match the energies obtained from photoelectron spectroscopy experiments as well as HF orbital energies do. The questions still being debated are how to assign similarities and how to physically interpret the differences.

A density functional is used to obtain the energy for the electron density. A functional is a function of a mathematic, in this case, the electron density. The exact density functional is not known. Therefore, there is a whole list of different functionals that may have advantages. Some of these functionals were developed from fundamental quantum mechanics and some were developed by parameterizing functions to best reproduce experimental results. Thus, there are in essence *ab initio* and semiempirical versions of DFT. DFT tends to be classified either as an *ab initio* method of a class by itself.

The advantage of using electron density is that the integrals for Coulomb repulsion need be done only over the electron density, which is a three- dimensional function, thus scaling as N^3. Furthermore, at least some electron correlation can be included in the calculation. These result in faster calculations than HF calculations (which scale as N^4) and computations those are a bit more accurate as well. The better DFT functionals give results with an accuracy similar to that of and MP2 calculation.

Density functionals can be broken down into several classes. The simplest is called the Xα method. This type of calculation includes electron exchange but not correlation. It was introduced by J.C. Slater, who in attempting to make an approximation to Hartree-Fock unwittingly discovered the simplest form of DFT. The Xα method is similar in accuracy to HF and sometimes better.

The simplest approximation to the complete problem is one based only on the electron density, called a local density approximation (LDA). For high spin systems, this is called the local spin density approximation (LSDA). LDA calculations have been widely used for band structure calculations. Their performance is less impressive for molecular calculations, where both qualitative and quantitative errors are encountered. For example, bonds tend to be too short and too strong. In recent years, LDA, LSDA, and VWN (the Vosko, Wilks, and Nusair functional) have become synonymous in the literature.

A more complex set of functionals utilizes the electron density and its gradient. These are called gradient-corrected methods. There are also hybrid methods that combine functionals from other methods with pieces of a Hartree-Fock calculation, usually the exchange integrals.

In general, gradient-corrected or hybrid calculations give the most accurate results. However, there are a few cased where Xα and LDA do quite well. LDA is known to give less accurate geometries and predicts binding energies significantly too large. The current generations of hybrid functionals are a bit more accurate than the present gradient-corrected techniques.

2.4.1 DFT exchange and correlations

In electronic structure calculations, E_{XC} is most commonly approximated within the local density approximation or generalized-gradient approximation. Ziegler, 1991 In the local density approximation (LDA), the value of $E_{xc}[\rho(r)]$ is approximated by the exchange-correlation energy of an electron in homogeneous electron gas of the same density $\rho(r)$, *i.e.*

$$E_{XC}^{LDA}[\rho(r)] = \int \epsilon_{XC}(\rho(r))\rho(r)dr \tag{2.10}$$

The most accurate data for $\epsilon_{XC}(\rho(r))$ is calculated from Quantum Monte Carlo calculations. For systems with slowly varying charge densities this approximation generally gives very good results. An obvious approach to improving the LDA, so called generalized gradient approximation (GGA), is to include gradient corrections by making E_{XC} a functional of the density and its gradient:

$$E_{XC}^{GGA}[\rho(r)] = \int \epsilon_{XC}(\rho(r))\rho(r)dr + \int F_{XC}[\rho(r), |\nabla\rho(r)|]dr \tag{2.11}$$

where F_{XC} is a correction chosen to satisfy one or several known limits for E_{XC}. Clearly, there is no unique recipe for the F_{XC}, and several functionals have been proposed in the literature. The development of improved functionals is currently a very active area of research and although incremental improvements are likely, it is far from clear whether the research will be successful in providing the substantial increase in accuracy that is desired.

2.4.2 Hybrid functionals

From the Hamiltonian equation and the definition of the exchange-correlation energy, an exact connection can be made between the E_{xc} and the corresponding potential connecting the non-interacting reference and the actual system. The resulting equation is called the ACF. Adiabatic connection formula and involves an integration over the parameter λ which turns on the electron-electron interaction

$$E_{XC} = \int_0^1 \langle \psi_\lambda | V_{XC}(\lambda) | \psi_\lambda \rangle d\lambda \tag{2.12}$$

In the λ=0 limit, the electrons are non-interacting and there is consequently no correlation. Since the Kohn-Sham wavefunction is simply a single Slater determinant of orbitals then if the KS orbitals are identical to the HF orbitals, the exact exchange energy is precisely the HF exchange energy:

$$E_X[\phi_i;\lambda=0] = -\frac{1}{2}\sum_{\sigma}\sum_{i,j}\int d^3r \int d^3r' \frac{\phi_{i\sigma}^*(r)\phi_{j\sigma}^*(r')\phi_{i\sigma}(r')\phi_{j\sigma}(r)}{|r-r'|} = E_X^{exact} \tag{2.13}$$

The approximation of exchange-correlation can be made by summing E_{XC} terms of different values of λ within the limit λ = 0 to 1. The choice of terms is arbitrary. Hybrid functionals includes a mixture of Hartree-Fock Exchange with DFT exchange-correlation.

B3LYP functional uses Becke's exchange functional with part of the Hartree-Fock exchange mixed in (Becke *[32])* and a scaling factor on the correlation part but using the LYP correlation function (Lee *et al. [33]*). The exchange-correlation energy has the form of

$$AE_X^{Slater} + (1-A)E_X^{HF} + B\Delta E_X^{Beck} + (1-C)E_C^{VWN} + CE_C^{LYP} \tag{2.14}$$

where the exchange includes the Slater exchange E_X^{Slater} , or local spin density exchange, along with corrections involving the gradient of the density and the correlation is provided by the LYP and VWN correlations. The constants *A*, *B*, and *C* are those determined by fitting to the G1 molecule set. The values of the three parameters are determined by fitting to the 56 atomization energies, 42 ionization potentials, 8 proton affinities, and 10 first-row atomic energies in the G1 molecule set, computing values of *A*=0.80, *B*=0.72, and *C*=0.81.

2.5 Transition State Theory and Statistical Mechanics

Transition state theory (TST) assumes that a reaction proceeded from one energy minimum to another via an intermediate maximum. The *transition state* is the configuration which divides the reactant and product parts of surface. For example, a molecule which has reached the transition state is continuing to product. The geometrical configuration of the energy maximum is called the *transition structure*. Within standard TST, the transition state and transition structure are identical, but this is not necessarily for more refined models. The direction of reaction coordinate is started from the reactant to product along a path where the energies are as low as possible and the TS is the point where the energy has a maximum. In the multidimensional case, TS is a first-order point on the potential energy surface as a maximum in the reaction coordinate direction and a minimum along all other coordinates.

Transition state theory assumes equilibrium energy distribution among all possible quantum states at all points along the reaction coordinates. The probability of finding a molecular in a given quantum state is proportional to $e^{-\Delta E/k_B T}$, which is Boltzman distribution. Assuming that the molecule at the TS is in equilibrium with the reactant, the macroscopic rate constant can be expressed as

$$k = \frac{k_B T e^{-\Delta G^{\neq}/RT}}{h} \tag{2.15}$$

in which $\Delta G^{\neq}$ is the Gibbs free energy difference between the TS and reactant, T is absolute temperature and k_B is Boltzmann's constant. It is clear that if the free energy of the reactant and TS can be calculated, the reactant rate follows trivially. The equilibrium constant for a reaction can be calculated from the free energy difference between the reactant and product.

$$K_{eq} = e^{-\Delta G_0 / RT} \tag{2.16}$$

The Gibbs free energy is given in terms of the enthalpy and entropy, $G = H - TS$. The enthalpy and entropy for a macroscopic ensemble of particles maybe calculated from properties of the individual molecules by means of statistical mechanics.

The energy of transition states is of crucial importance for the rate of chemical reactions. However, the vary nature of transition states means that it is not possible to observe them directly. Hammond's postulate allows to making assumption about the structure of transition states. In a publication in the Journal of the American Chemical Society, Hammond postulated that “If two states, as for example a transition state and an unstable intermediate, occur consecutively during a reaction process and have nearly the same energy content, their interconversion will only involve a small reorganization of molecular structure” *[34-35]*. That is, along the reaction coordinate, species with similar energies also have similar structures. Hammond postulated that in highly exothermic reactions the transition state is structurally similar to the reactant, but that in highly endothermic reactions the product is a better model of the transition state. The caution against using the postulate is that if reactions are more thermoneutral or slightly exothermic reaction, the transition is resembled neither reactant nor product.

CHAPTER III

DETAIL OF THE CALCULATION

3.1 Methods of calculations

The standard enthalpy ΔH^O and Gibbs free energy changes ΔG^O of conversion reactions of this system have been derived from the frequency calculations. The rate constant k(T) derived from transition state theory was computed from activation free energy, $\Delta^{\ddagger}G^O$ by

$$k(T) = \frac{k_B T}{hc^o} \exp(-\Delta^{\ddagger}G^O/RT) \tag{3.1}$$

where concentration factor, c^o of unity is used, k_B is Boltzmann's constant, h is Plank's constant, T is the absolute temperature and R is gas constant. The above formula was employed to compute the reaction rate constants for corresponding activation free energies.

The pinacol rearrangement of 2,3-dimethyl-2,3-butanediol, 2,3-dimethyl-2,3-pentanediol in acid catalyst, full geometry optimizations were computed by density functional theory (DFT). Density functional calculations have been performed with the Becke's three parameters hybrid density function using the Lee, Yang and Parr correlation functional (B3LYP). All geometry optimizations have been carried out use the hybrid density functional B3LYP with the 6-31G(d) and 6-311+G(d,p) basis sets. The energies of the B3LYP/6-31G(d) and B3LYP/6-311+G(d,p) optimized-geometries have been calculated with the zero-point energy corrections. The transition states were confirmed by one imaginary frequency. The intrinsic reaction coordinate (IRC) method was used to track minimum energy paths from transition structures to the corresponding minimum.

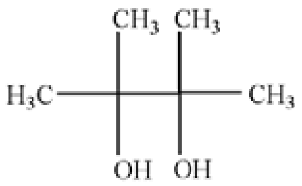

(a)

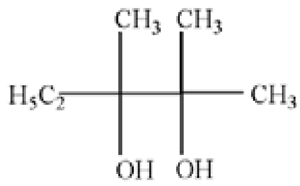

(b)

Figure 3.1 Structures of (a) 2,3-dimethyl-2,3-butanediol (b) 2,3-dimethyl-2,3-pentanediol.

In this study two reactants were investigated: 2,3-dimethyl-2,3-butanediol and 2,3-dimethyl-2,3-pentanediol (see Figure 3.1). For pinacol rearrangement of 2,3-dimethyl-2,3-butanediol acid-catalyzed models with respect to the increased numbers of hydration water were investigated for the effect of hydration water to product compositions. Model I is an acid-catalyzed model of a gas-phase system which is composed of one proton as acid catalytic atom without hydration water except dehydration water which is released from the reaction. Model II is an acid-catalyzed model of which the reactant is protonated by a single proton of which the molecule is hydrated by one water molecule. For pinacol rearrangement of 2,3-dimethyl-2,3-pentanediol in acid catalyst, the structure geometries were calculated in the same way like 2,3-dimethyl-2,3-butanediol reactant and compare result of both of them.

The structures of 2,3-dimethyl-2,3-butanediol, 2,3-dimethyl-2,3-pentanediol, intermediates transition states, 2,3-dimethyl-1,3-butadiene and 2,3-dimethyl-1,3-pentadiene were optimized by Density Functional Theory (DFT) calculations using 6-31G(d) and 6-311+G(d,p) basis sets. The structural energies of 2,3-dimethyl-2,3-butanediol, 2,3-dimethyl-2,3-pentanediol, intermediates and transition states were computed at B3LYP/6-31G(d) and B3LYP/6-311+G(d,p) level of theory. The transition states were confirmed by imaginary frequency. the transition structures of all related species have been located using the B3LYP/6-31G(d) optimized transition states. The reaction energy ΔE^{o}_{298}, standard enthalpy ΔH^{o}_{298} and Gibbs free energy changes ΔG^{o}_{298} of all reactions have been derived from the frequency calculations at B3LYP/6-31G(d) and B3LYP/6-311+G(d,p) level of theory. The reaction energy All structure optimizations and energy calculations were performed with the GAUSSIAN 03 program.*[36]* The MOLDEN 3.7 program*[37]* was utilized to display molecular structures and observe the geometry convergence via the Gaussian output files. The molecular graphics of all species were generated with the Molekel 4.3 program.*[38]*

CHAPTER IV

RESULTS AND DISCUSSION

This chapter is the results of conversion reactions of 2,3-dimethyl-2,3-butanediol (DMBDOL) to 2,3-dimethyl-1,3-butadiene (DMBDENE) and 2,3-dimethyl-2,3-pentanediol (DMPDOL) to 2,3-dimethyl-1,3-pentadiene (DMPDENE) were investigated by acid-catalyzed on pinacol rearrangement reaction. Relative energies and thermodynamic properties of the various models are shown below. All structures conversion in pinacol rearrangement reaction were optimized using DFT at B3LYP/6-31G(d) and B3LYP/6-311+G(d,p) level of theory. The zero point energies and thermodynamic quantities of activation steps were derived from the frequency calculations at 298.15 K at the B3LYP/6-31G(d) and B3LYP/6-311+G(d,p) level of theory too.

4.1 Conversion of 2,3-dimethyl-2,3-butanediol.

Reaction mechanisms of 2,3-dimethyl-2,3-butanediol (DMBDOL) conversion to 2,3-dimethyl-1,3-butadiene of acid-catalyzed water-addition models of concerted pathways are found. Total energies and geometrical structures and the corresponding transition states of various acid-catalyzed models are determined at the B3LYP/6-31G(d) and B3LYP/6-311+G(d,p) level of theory with zero point energy corrections.

The alternative pinacol rearrangement leading 2,3-dimethy-1,3-butadiene (Fig 4.1) proceeds via protonation of the hydroxyl group and subsequent loss of water to afford the stable carbocation, which can lose a proton to form 2,3-dimethyl-3-butene-2-ol. Protonation of the hydroxyl group in 2,3-dimethyl-3-butene-2-ol and loss of water leads to allylic carbocation that leading to 2,3-dimethyl-1,3-butadiene as the main elimination product.

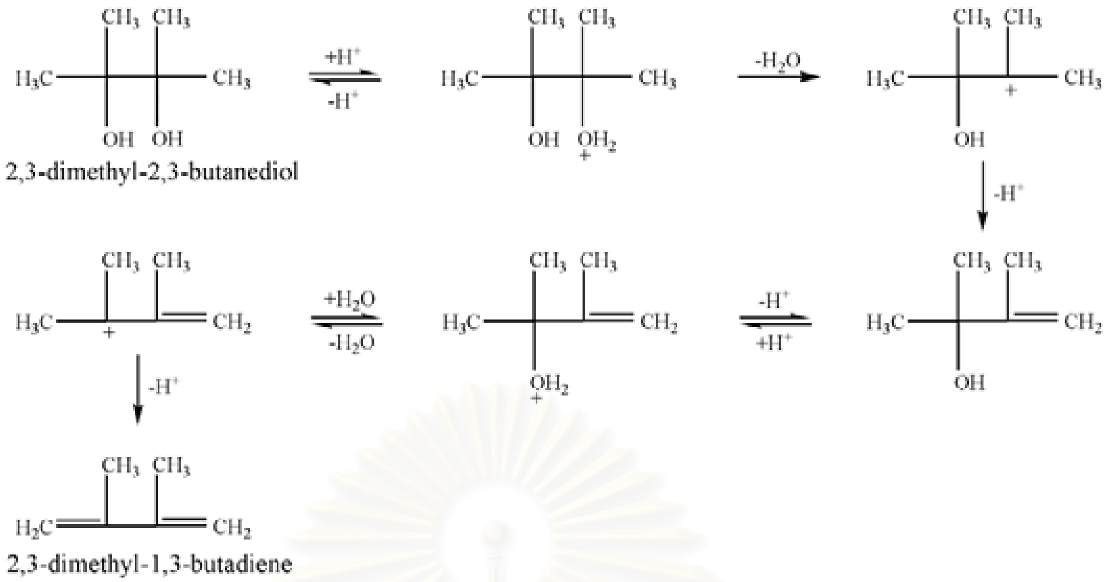

Figure 4.1 The conversion pathway of 2,3-dimethy-2,3-butanediol to 2,3-dimethy-1,3-butadiene.

In this work, the acid-catalyzed models for the pinacol rearrangement of 2,3-dimethyl-2,3-butanediol are studied. The first model, model I, is the gas phase model whilst the model II is the models which water molecules are added. Model II is added one water molecule. Relative energies and thermodynamic quantities of acid-catalyzed reaction of method B3LYP/6-31G(d) and B3LYP/6-311+G(d,p) for models I and II are shown in Tables 4.1, 4.2, 4.3 and 4.4 respectively.

The potential energies diagrams of pinacol rearrangement mechanisms of conversion reaction of 2,3-dimethyl-2,3-butanediol (DMBDOL) model I and model II (with one water molecule) computed at B3LYP/6-31G(d) and B3LYP/6-311+G(d,p) levels of theory are shown in Figure 4.3, 4.5, 4.7 and 4.9 respectively. 2,3-dimethyl-2,3-butanediol, intermediates transition states, 2,3-dimethyl-1,3-butadiene are shown in Figures 4.2, 4.4, 4.6 and 4.8 respectively. Of those figures, the O—H distances of hydrogen bond of intermolecular interaction between water molecules and involved species are shown. From these results support the acknowledgement that pinacol rearrangements in acid catalyst in aqueous phase are occurred rapidly.

Table 4.1 Reaction energies and thermodynamic quantities of 2,3-dimethyl-2,3-butanediol conversion, computed at the B3LYP/6-31G(d) level of theory

Reactions /systems	ΔE^{a}	ΔG^{o}_{298} ^{a}	ΔH^{o}_{298} ^{a}	K_{298}
DMBDOL + H^+ $\rightarrow$ INT1	-206.48	-206.31	-206.56	1.74 X 10^{151}
INT1 $\rightarrow$ TS1 $\rightarrow$ INT2	5.52	2.83	6.92	8.45 X 10^{-3}
INT2 $\rightarrow$ TS2 $\rightarrow$ INT3	9.32	7.74	9.79	2.13 X 10^{-6}
INT3 $\rightarrow$ H_2O + H_3O^+ + DMBDENE	-68.01	-84.66	-66.97	1.15 X 10^{62}

^{a} In kcal mol^{-1}.

Table 4.2 Reaction energies and thermodynamic quantities of 2,3-dimethyl-2,3-butanediol conversion in system with a water molecule, computed at the B3LYP/6-31G(d) level of theory

Reactions /systems	ΔE^{a}	ΔG^{o}_{298} ^{a}	ΔH^{o}_{298} ^{a}	K_{298}
DMBDOL + H_2O +H^+ $\rightarrow$ INT1 + H_2O	-206.48	-206.31	-206.56	1.74 X 10^{151}
INT1 + H_2O $\rightarrow$ INT1´	-22.35	-13.96	-22.80	1.71 X 10^{10}
INT1´ $\rightarrow$ TS1´ $\rightarrow$ INT2´	9.16	7.76	9.63	2.03 X 10^{-6}
INT2´ $\rightarrow$ TS2´ $\rightarrow$ INT3´	11.68	8.61	12.50	4.89 X 10^{-7}
INT3´ $\rightarrow$ 2H_2O + H_3O^+ + DMBDENE	-183.30	-174.45	-188.33	7.75 X 10^{127}

^{a} In kcal mol^{-1}.

Table 4.3 Reaction energies and thermodynamic quantities of 2,3-dimethyl-2,3-butanediol conversion, computed at the B3LYP/6-311+G(d,p) level of theory

Reactions /systems	ΔE [a]	ΔG^{o}_{298} [a]	ΔH^{o}_{298} [a]	K_{298}
DMBDOL + H^+ → INT1	-204.01	-204.06	-203.73	3.91 X 10^{149}
INT1 → TS1 → INT2	-2.35	-5.03	-0.98	4.87 X 10^{3}
INT2 → TS2 → INT3	5.67	5.19	5.63	4.68 X 10^{-4}
INT3 → H_2O + H_3O^+ + DMBDENE	-85.23	-102.91	-83.71	2.75 X 10^{75}

[a] In kcal mol^{-1}.

Table 4.4 Reaction energies and thermodynamic quantities of 2,3-dimethyl-2,3-butanediol conversion in system with a water molecule, computed at the B3LYP/6-311+G(d,p) level of theory

Reactions /systems	ΔE [a]	ΔG^{o}_{298} [a]	ΔH^{o}_{298} [a]	K_{298}
DMBDOL + H_2O +H^+ → INT1 + H_2O	-204.01	-204.06	-203.73	3.91 X 10^{149}
INT1 + H_2O → INT1´	-18.76	-10.63	-19.09	6.25 X 10^{7}
INT1´ → TS1´ → INT2´	2.10	-0.96	3.25	5.06
INT2´ → TS2´ → INT3´	2.84	0.42	3.54	4.9 X 10^{-1}
INT3´ → 2H_2O + H_3O^+ + DMBDENE	-101.69	-107.49	-91.58	1.37 X 10^{67}

[a] In kcal mol^{-1}.

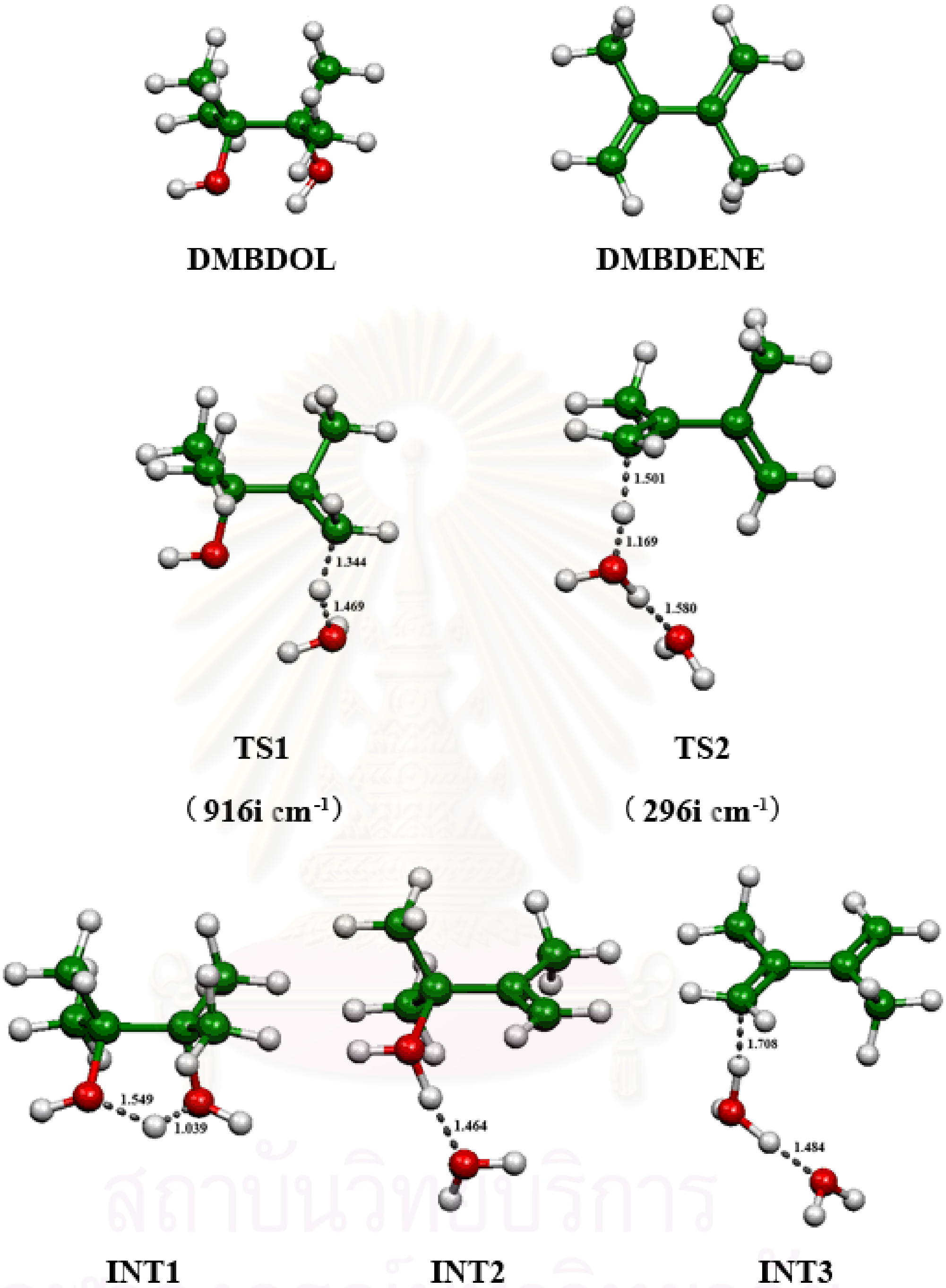

Figure 4.2 The B3LYP/6-31G(d) optimized geometries of conversion reaction of 2,3-dimethyl-2,3-butanediol, 2,3-dimethyl-1,3-butadiene, intermediates and transition states. Hydrogen bond distances are in angstrom. Values in parenthesis are imaginary frequencies.

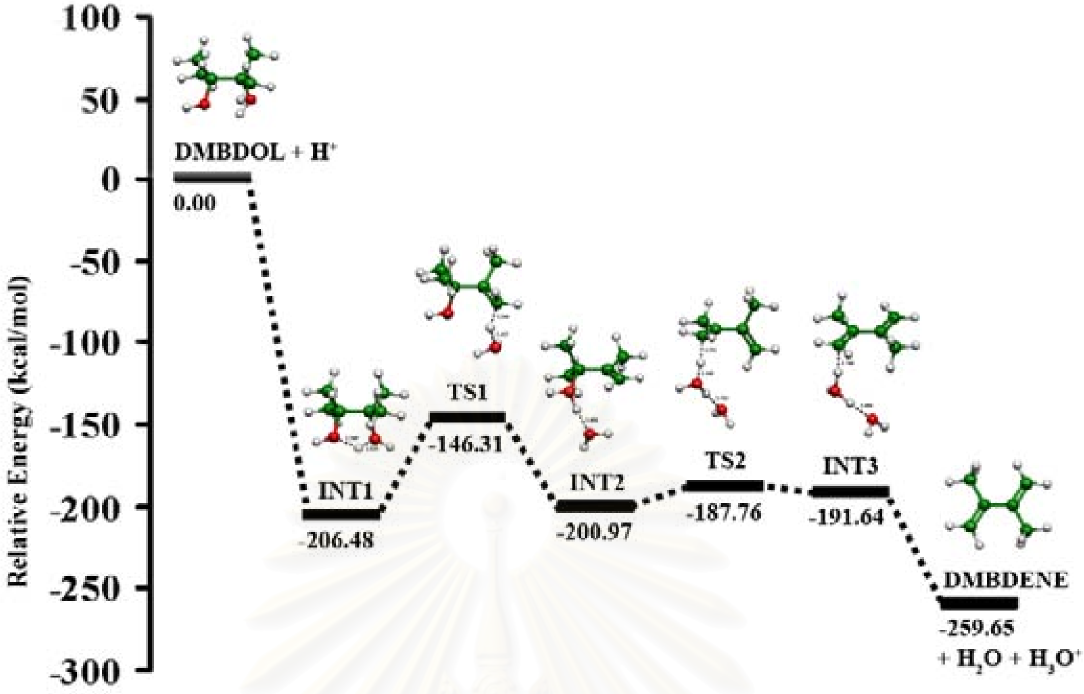

Figure 4.3 Relative energetic profile of conversion reaction of 2,3-dimethyl-2,3-butanediol (DMBDOL). All energies are based upon B3LYP/6-31G(d) total energies of DMBDOL.

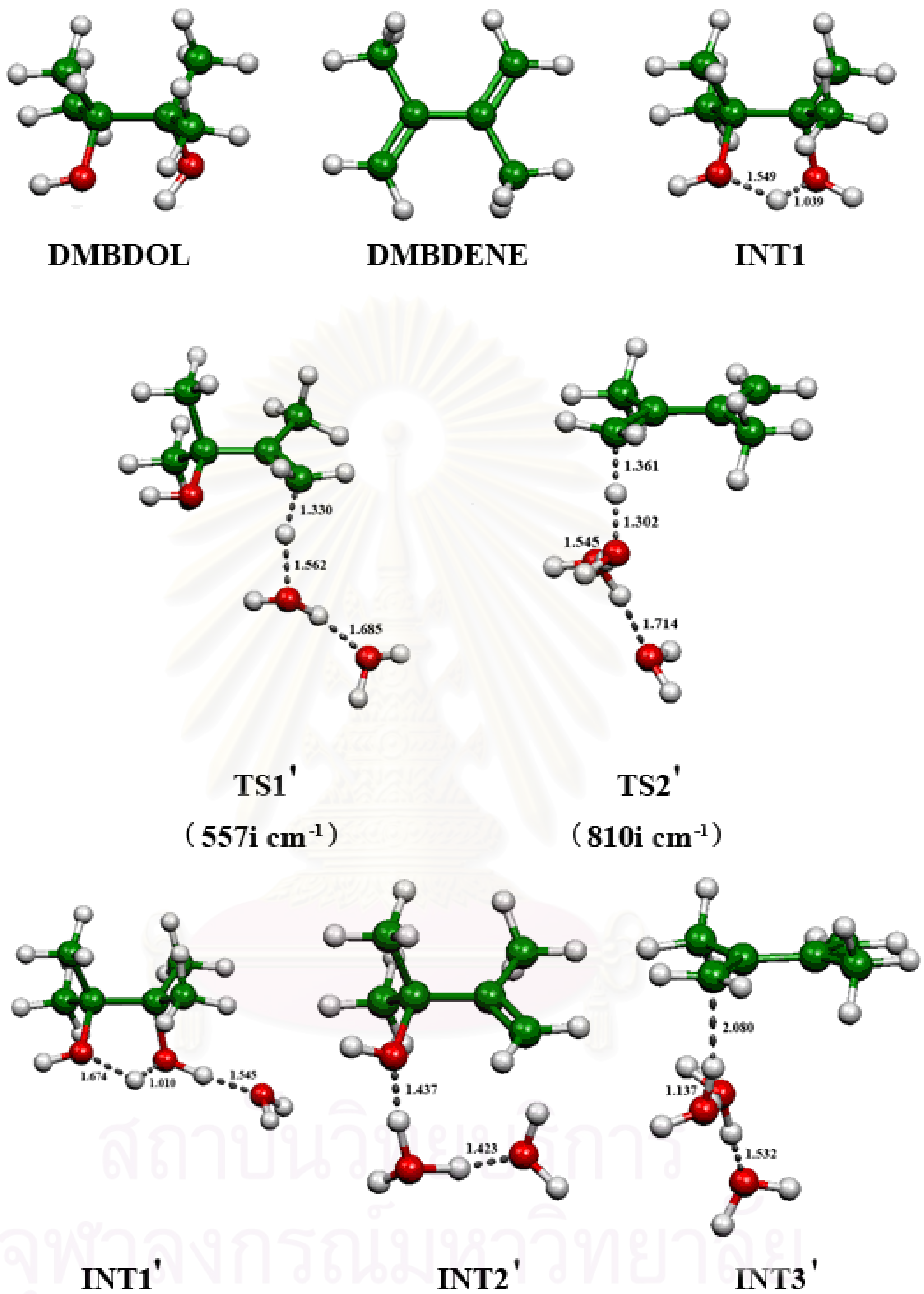

Figure 4.4 The B3LYP/6-31G(d) optimized geometries of conversion reaction of 2,3-dimethyl-2,3-butanediol, 2,3-dimethyl-1,3-butadiene, intermediates and transition states in system with a water molecule. Hydrogen bond distances are in angstrom. Values in parenthesis are imaginary frequencies.

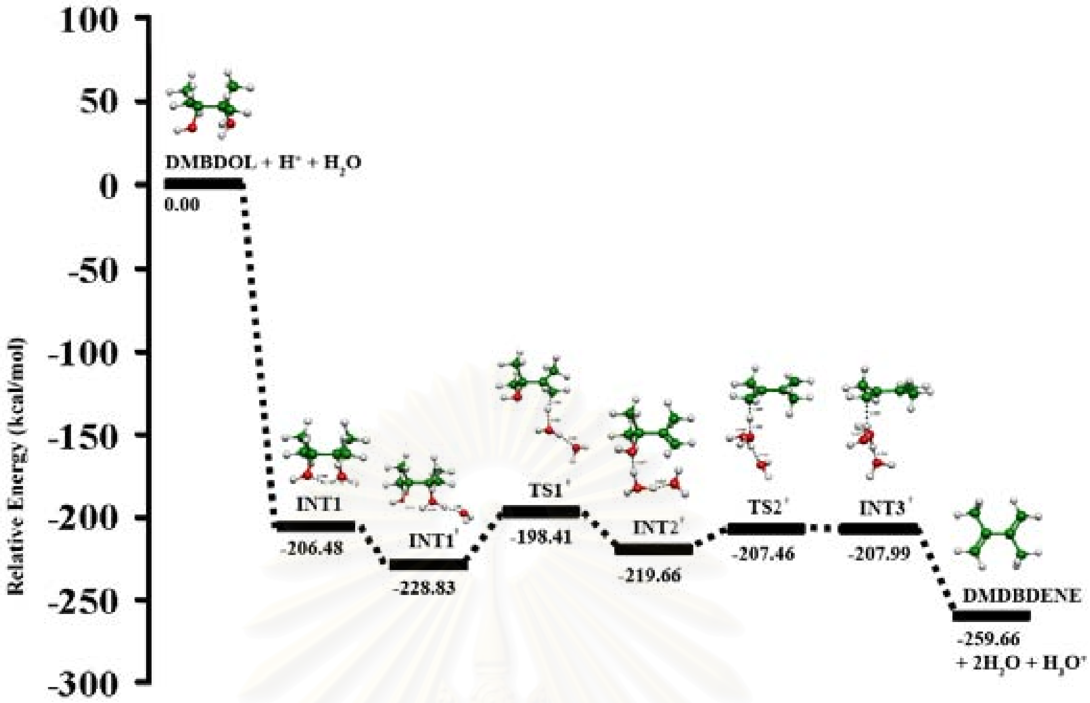

Figure 4.5 Relative energetic profile of conversion reaction of 2,3-dimethyl-2,3-butanediol (DMBDOL) in system with a water molecule. All energies are based upon B3LYP/6-31G(d) total energies of DMBDOL.

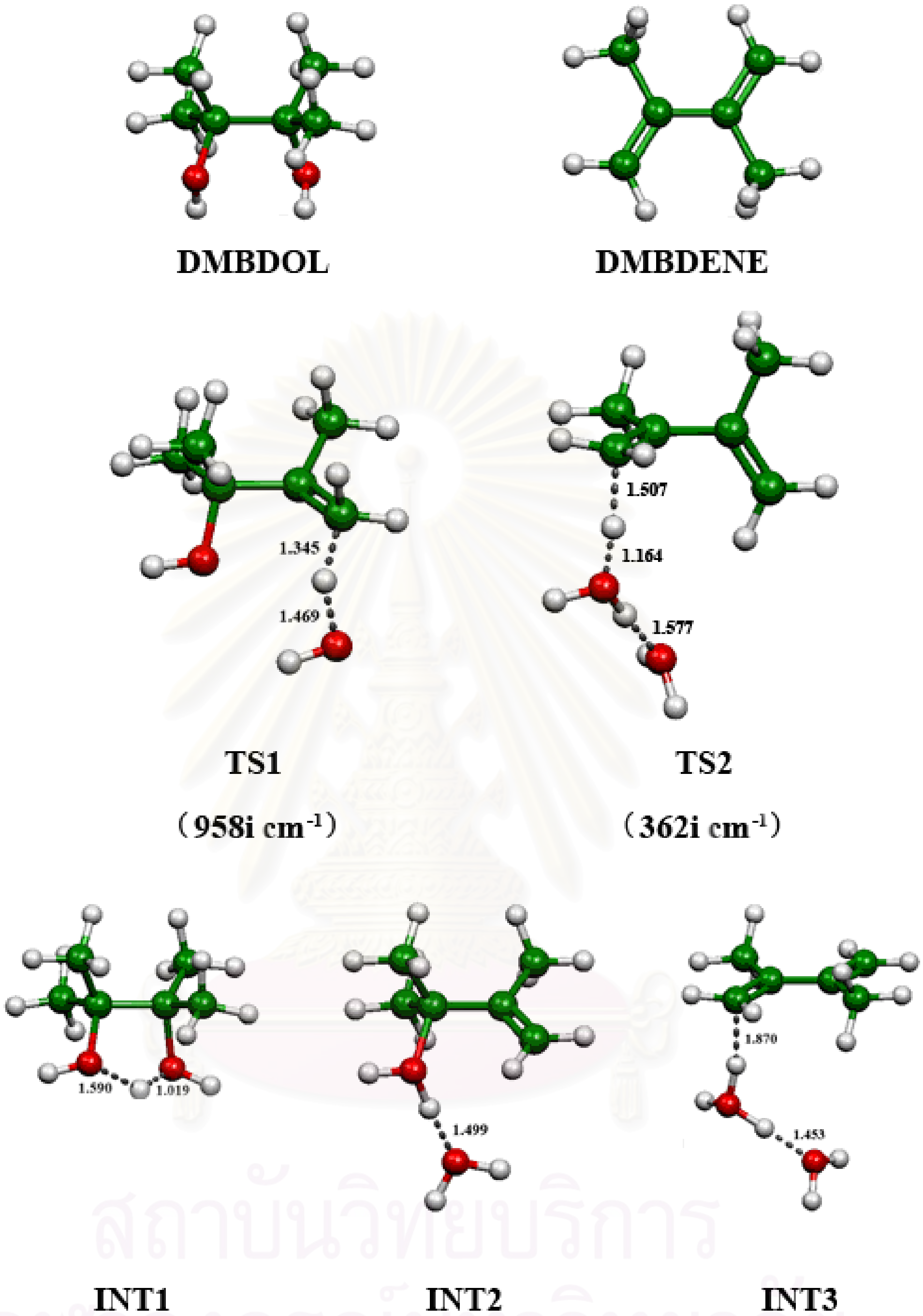

Figure 4.6 The B3LYP/6-311+G(d.p) optimized geometries of conversion reaction of 2,3-dimethyl-2,3-butanediol, 2,3-dimethyl-1,3-butadiene, intermediates and transition states. Hydrogen bond distances are in angstrom. Values in parenthesis are imaginary frequencies.

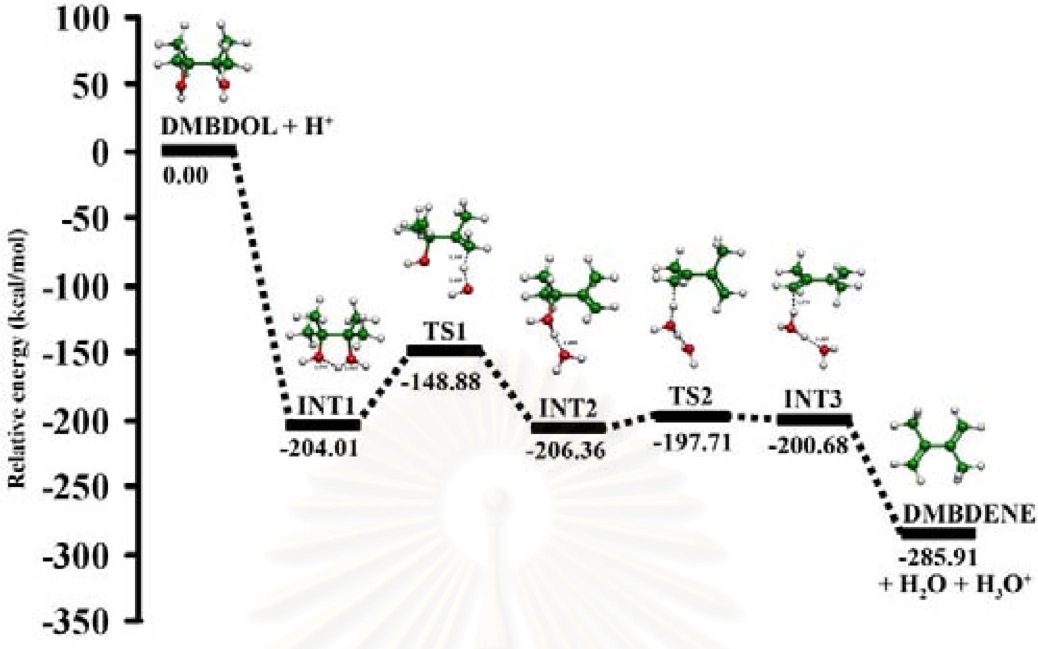

Figure 4.7 Relative energetic profile of conversion reaction of 2,3-dimethyl-2,3-butanediol (DMBDOL). All energies are based upon B3LYP/6-311+G(d,p) total energies of DMBDOL.

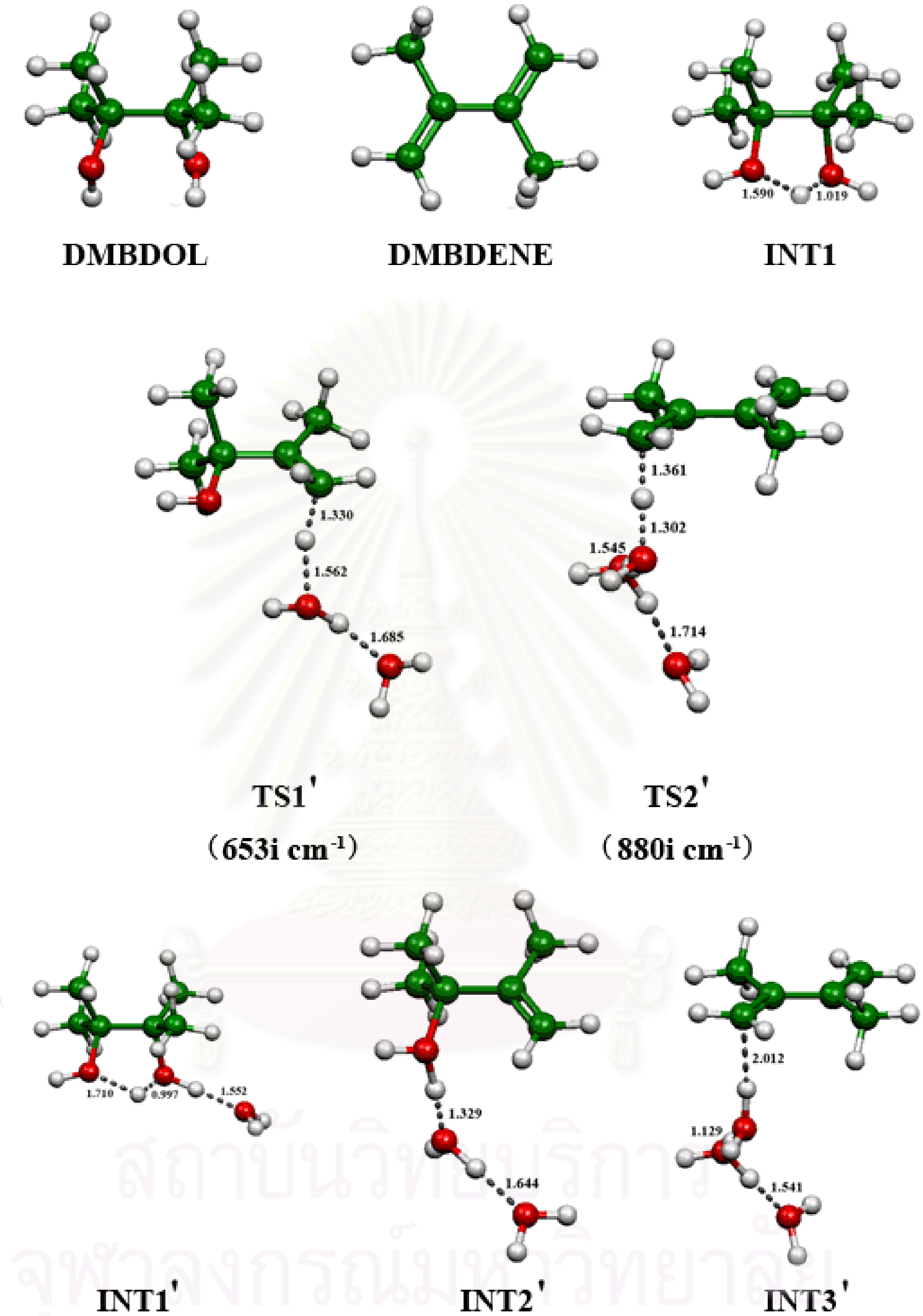

Figure 4.8 The B3LYP/6-311+G(d,p) optimized geometries of conversion reaction of 2,3-dimethyl-2,3-butanediol, 2,3-dimethyl-1,3-butadiene, intermediates and transition states in system with a water molecule. Hydrogen bond distances are in angstrom. Values in parenthesis are imaginary frequencies.

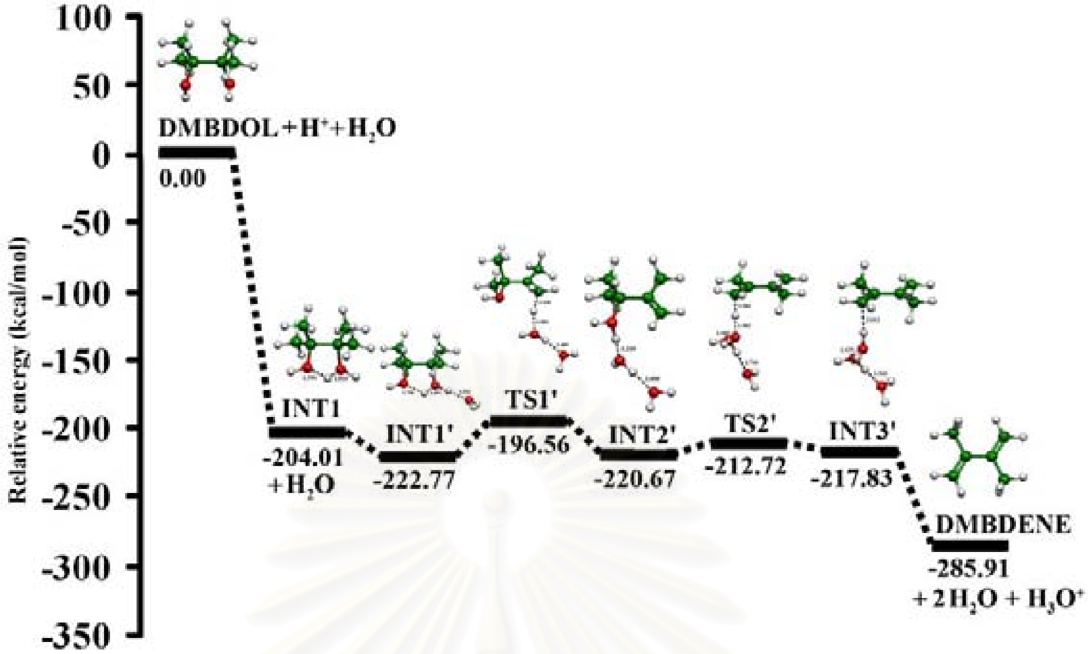

Figure 4.9 Relative energetic profile of conversion reaction of 2,3-dimethyl-2,3-butanediol (DMBDOL) in system with a water molecule. All energies are based upon B3LYP/6-311+G(d,p) total energies of DMBDOL.

4.2 Conversion of 2,3-dimethyl-2,3-pentanediol.

Reaction mechanisms of 2,3-dimethyl-2,3-pentanediol (DMBPOL) conversion to 2,3-dimethyl-1,3-pentadiene of acid-catalyzed water-addition models of concerted pathways are found. Total energies and geometrical structures and the corresponding transition states of various acid-catalyzed models are determined at the B3LYP/6-31G(d) and B3LYP/6-311+G(d,p) level of theory with zero point energy corrections.

The alternative pinacol rearrangement leading 2,3-dimethy-1,3-pentadiene (Fig 4.10) proceeds via protonation of the hydroxyl group and subsequent loss of water to afford the stable carbocation, which can lose a proton to form 2,3-dimethyl-3-pentene-2-ol. Protonation of the hydroxyl group in 2,3-dimethyl-3-pentene-2-ol and loss of water leads to allylic carbocation that leading to 2,3-dimethyl-1,3-pentadiene as the main elimination product.

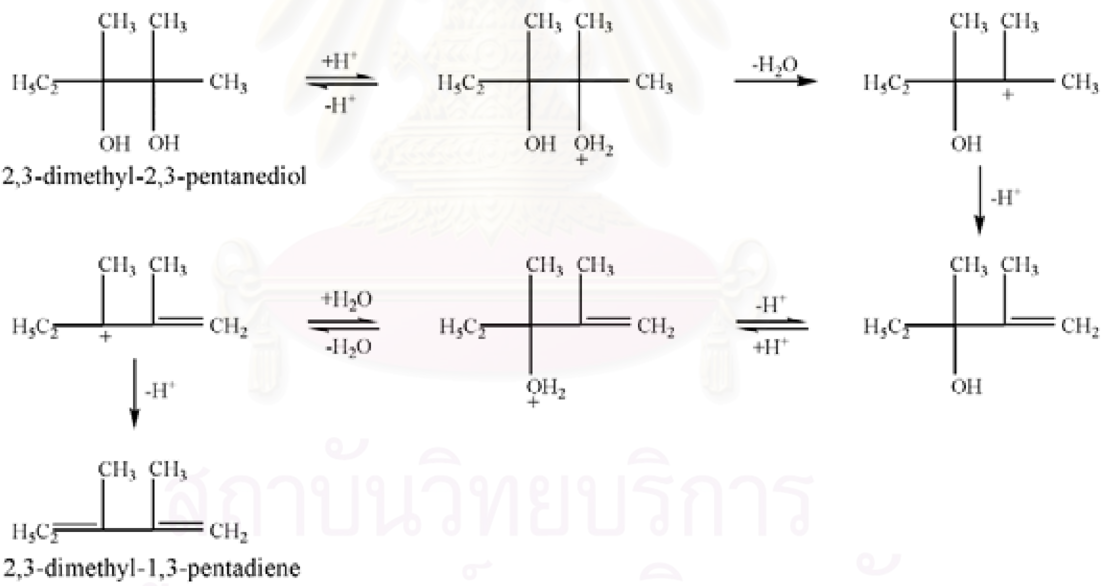

Figure 4.10 The conversion pathways of 2,3-dimethy-2,3-pentanediol to 2,3-dimethy-1,3-pentadiene.

The acid-catalyzed models for the pinacol rearrangement of 2,3-dimethyl-2,3-pentanediol are studied. The model III is the gas phase model whilst the model IV is the models which water molecules are added. Model IV is added one water molecule. Relative energies and thermodynamic quantities of acid-catalyzed reaction of method

B3LYP/6-31G(d) and B3LYP/6-311+G(d,p) for models III and IV are shown in Tables 4.5, 4.6, 4.7 and 4.8 respectively.

The potential energies diagrams of pinacol rearrangement mechanisms of conversion reaction of 2,3-dimethyl-2,3-pentanediol (DMPDOL) model III and model IV (with one water molecule) computed at B3LYP/6-31G(d) and B3LYP/6-311+G(d,p) levels of theory are shown in Figure 4.12, 4.14, 4.16 and 4.18 respectively. 2,3-dimethyl-2,3-pentanediol, intermediates transition states, 2,3-dimethyl-1,3-pentadiene are shown in Figures 4.11, 4.13, 4.15 and 4.17 respectively. Of those figures, the O—H distances of hydrogen bond of intermolecular interaction between water molecules and involved species are shown.

Table 4.5 Reaction energies and thermodynamic quantities of 2,3-dimethyl-2,3-pentanediol conversion, computed at the B3LYP/6-31G(d) level of theory

Reactions /systems	ΔE [a]	ΔG^{o}_{298} [a]	ΔH^{o}_{298} [a]	K_{298}
DMPDOL + H^+ → INT1	-207.08	-206.91	-207.70	4.80×10^{151}
INT1 → TS1 → INT2	5.81	3.59	6.94	2.33×10^{-3}
INT2 → TS2 → INT3	8.57	7.10	8.79	6.24×10^{-6}
INT3 → H_2O + H_3O^+ + DMPDNE	-157.45	-152.25	-160.12	4.06×10^{111}

[a] In kcal mol^{-1}.

Table 4.6 Reaction energies and thermodynamic quantities of 2,3-dimethyl-2,3-pentanediol conversion in system with a water molecule, computed at the B3LYP/6-31G(d) level of theory

Reactions /systems	ΔE [a]	ΔG^{o}_{298} [a]	ΔH^{o}_{298} [a]	K_{298}
DMPDOL + H_2O +H^+ → INT1 + H_2O	-207.08	-206.91	-207.70	4.80×10^{151}
INT1 + H_2O → INT1´	-21.97	-13.53	-21.86	8.27×10^{9}
INT1´ → TS1´ → INT2´	9.36	7.06	10.15	6.63×10^{-6}
INT2´ → TS2´ → INT3´	8.27	3.23	9.30	4.31×10^{-3}
INT3´ → 2H_2O + H_3O^+ + DMPDENE	-180.80	-169.30	-180.42	1.30×10^{124}

[a] In kcal mol^{-1}.

Table 4.7 Reaction energies and thermodynamic quantities of 2,3-dimethyl-2,3-pentanediol conversion, computed at the B3LYP/6-311+G(d,p) level of theory

Reactions /systems	ΔE [a]	ΔG^{o}_{298} [a]	ΔH^{o}_{298} [a]	K_{298}
DMPDOL + H^+ → INT1	-205.34	-204.73	-205.47	1.20×10^{150}
INT1 → TS1 → INT2	-0.39	-3.73	1.06	5.46×10^{2}
INT2 → TS2 → INT3	0.88	0.09	0.99	8.65×10^{-1}
INT3 → H_2O + H_3O^+ + DMPDENE	-105.39	-99.74	-108.34	1.32×10^{73}

[a] In kcal mol^{-1}.

Table 4.6 Reaction energies and thermodynamic quantities of 2,3-dimethyl-2,3-pentanediol conversion in system with a water molecule, computed at the B3LYP/6-311+G(d,p) level of theory

Reactions /systems	ΔE [a]	ΔG^{o}_{298} [a]	ΔH^{o}_{298} [a]	K_{298}
DMPDOL + H_2O +H^+ → INT1 + H_2O	-205.34	-204.73	-205.47	1.20×10^{150}
INT1 + H_2O → INT1´	-18.32	-10.08	-18.10	2.44×10^{7}
INT1´ → TS1´ → INT2´	2.59	0.61	3.23	3.56×10^{-1}
INT2´ → TS2´ → INT3´	0.51	-2.11	1.27	3.52×10^{1}
INT3´ → 2H_2O + H_3O^+ + DMBDENE	-100.75	-91.82	-106.13	2.04×10^{67}

[a] In kcal mol^{-1}.

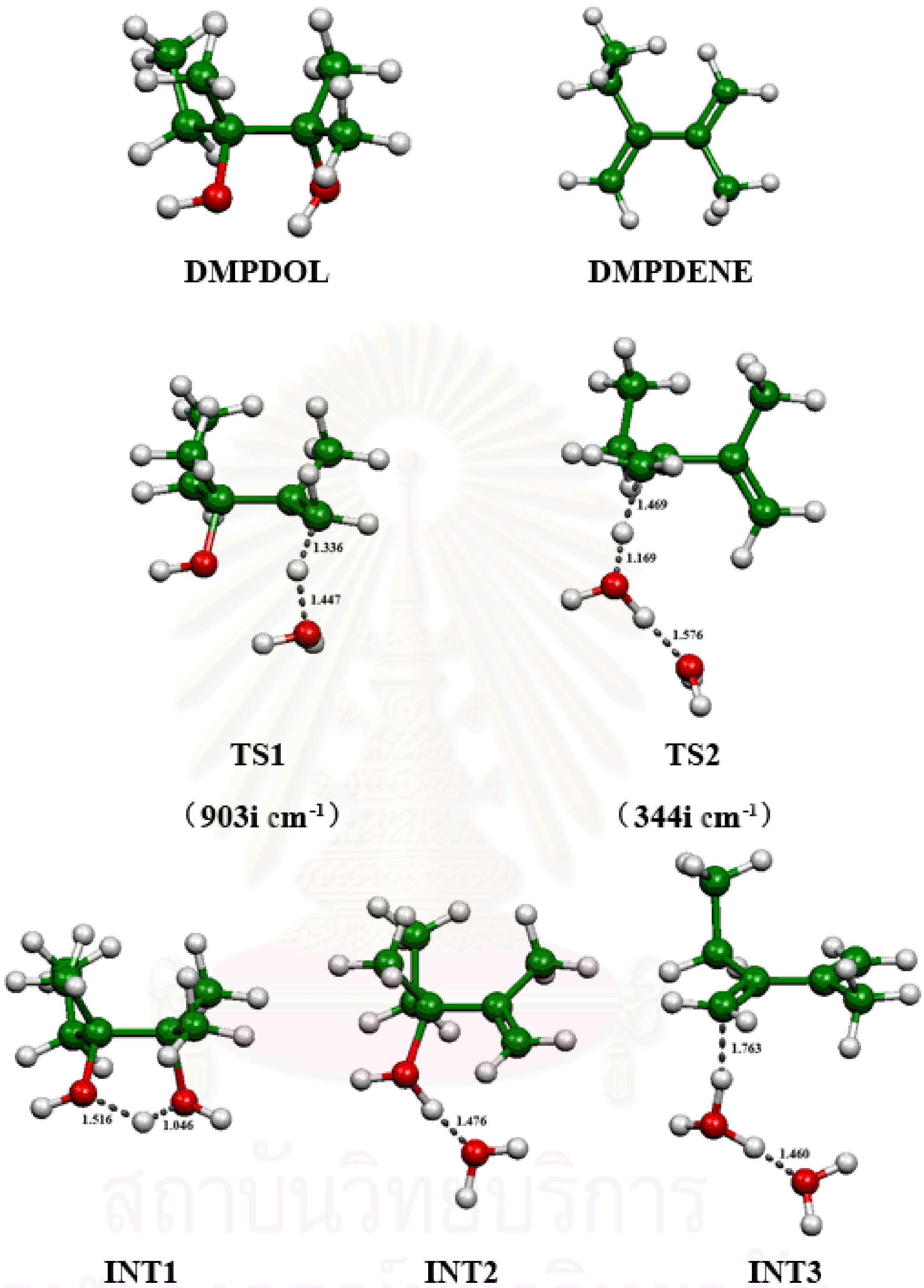

Figure 4.11 The B3LYP/6-31G(d) optimized geometries of conversion reaction of 2,3-dimethyl-2,3-pentanediol, 2,3-dimethyl-1,3-pentadiene, intermediates and transition states. Hydrogen bond distances are in angstrom. Values in parenthesis are imaginary frequencies.

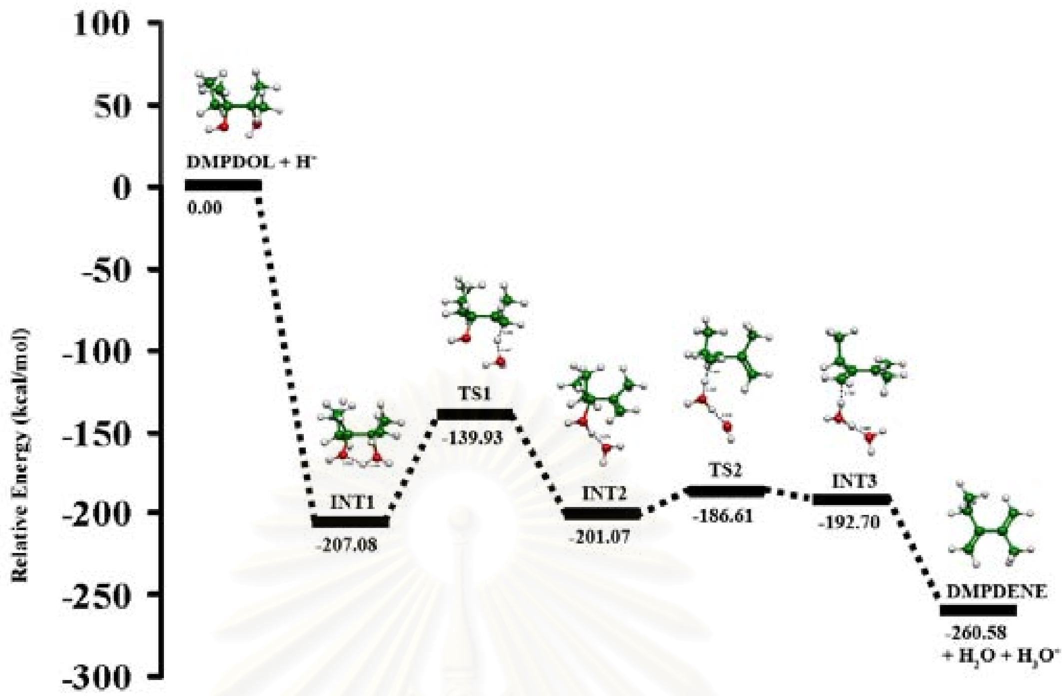

Figure 4.12 Relative energetic profile of conversion reaction of 2,3-dimethyl-2,3-pentanediol (DMPDOL). All energies are based upon B3LYP/6-31G(d) total energies of DMPDOL.

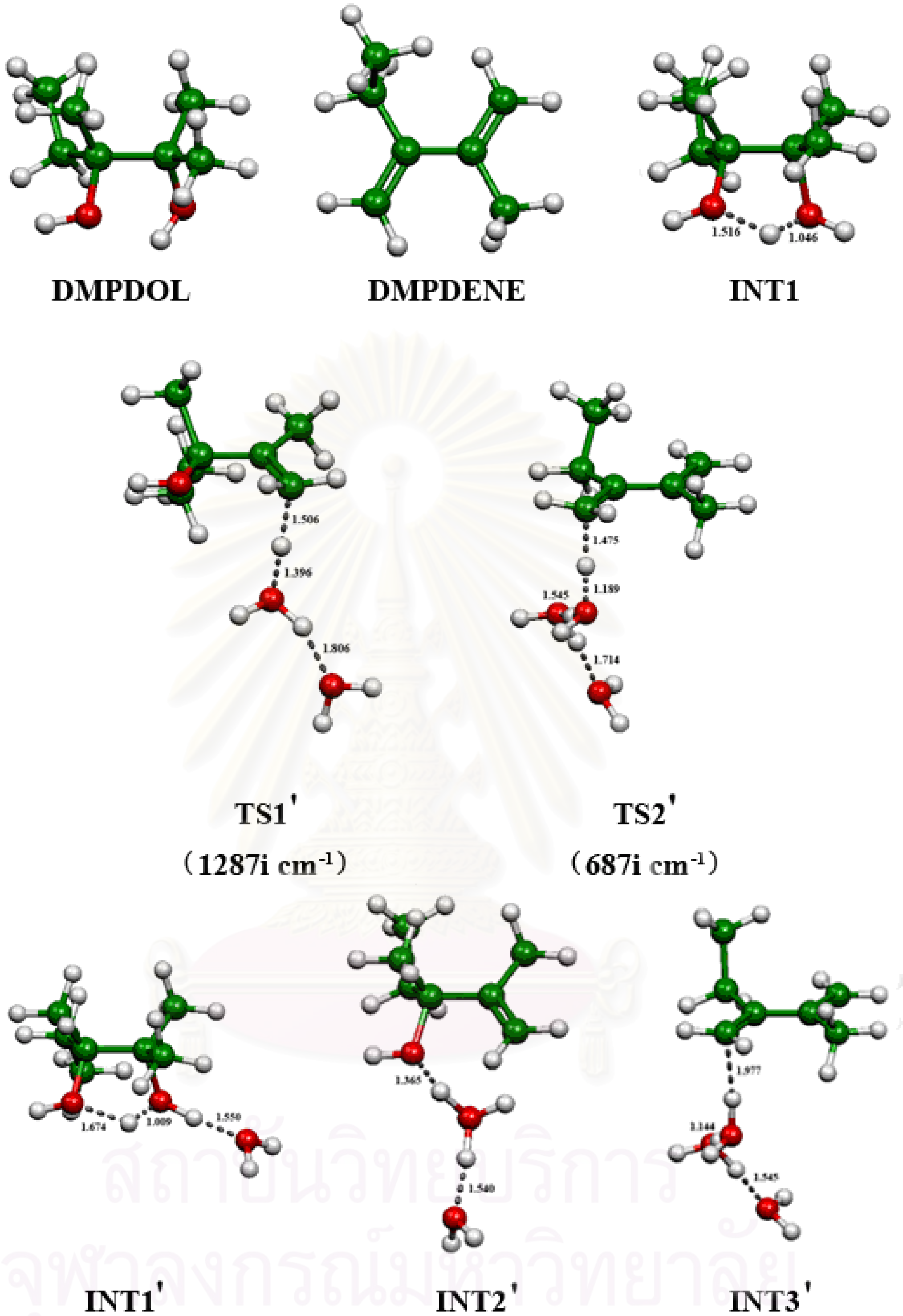

Figure 4.13 The B3LYP/6-31G(d) optimized geometries of conversion reaction of 2,3-dimethyl-2,3-pentanediol, 2,3-dimethyl-1,3-pentadiene, intermediates and transition states in system with a water molecule. Hydrogen bond distances are in angstrom. Values in parenthesis are imaginary frequencies.

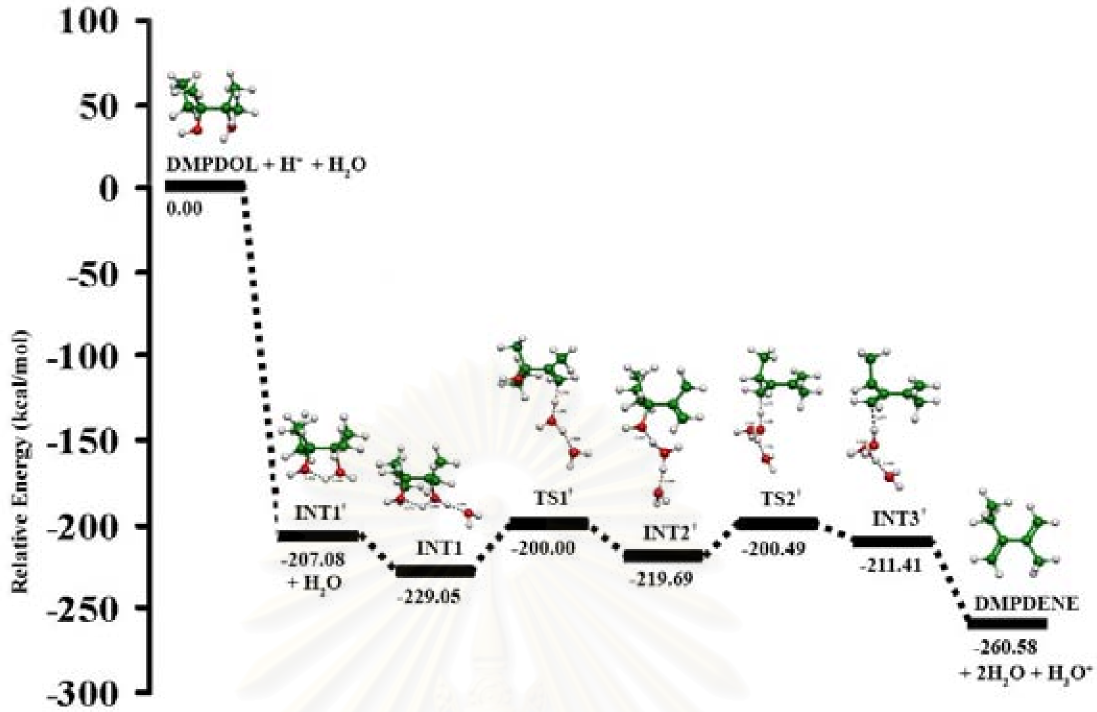

Figure 4.14 Relative energetic profile of conversion reaction of 2,3-dimethyl-2,3-pentanediol (DMPDOL) in system with a water molecule. All energies are based upon B3LYP/6-31G(d) total energies of DMPDOL.

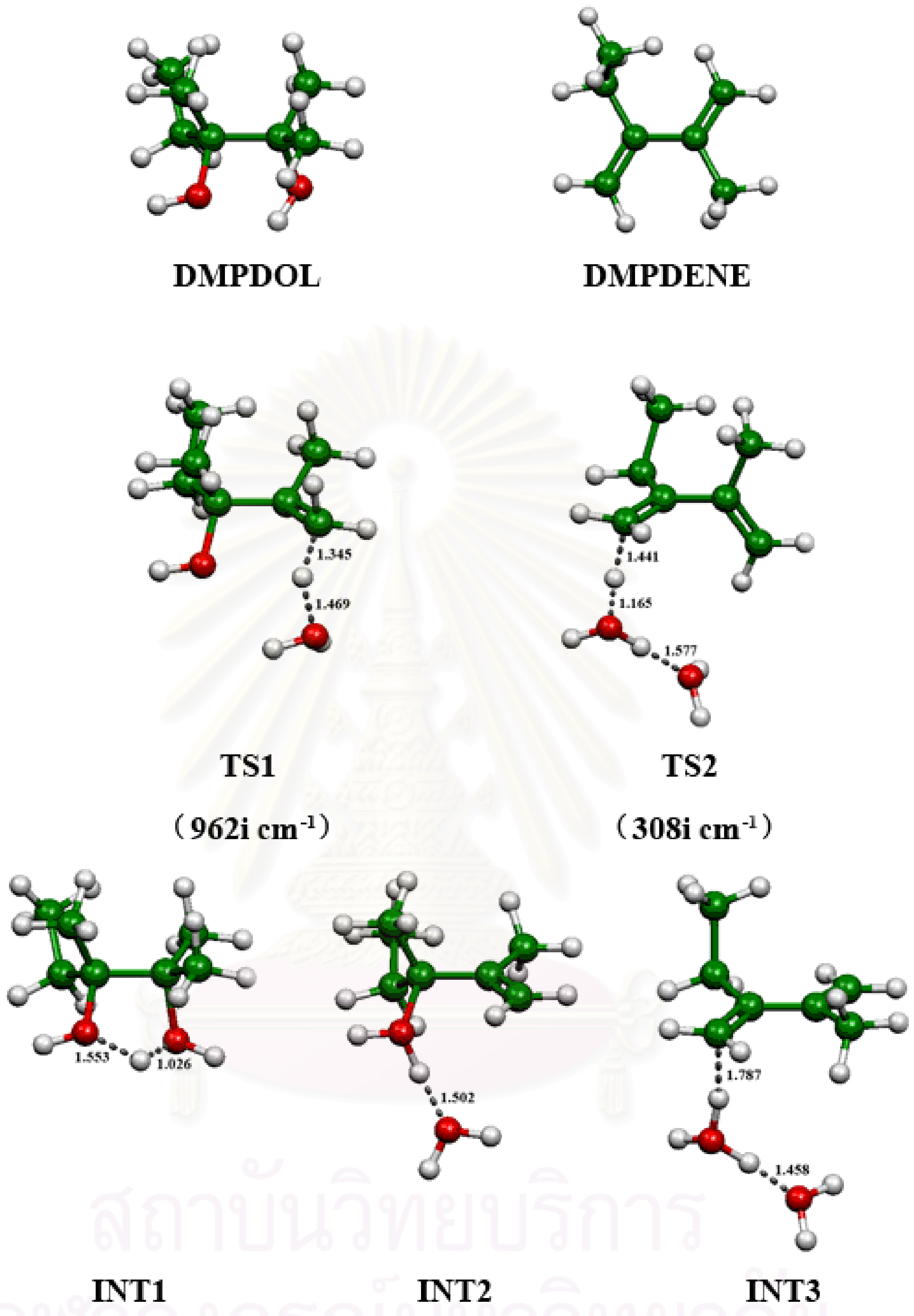

Figure 4.15 The B3LYP/6-311+G(d,p) optimized geometries of conversion reaction of 2,3-dimethyl-2,3-pentanediol, 2,3-dimethyl-1,3-pentadiene, intermediates and transition states. Hydrogen bond distances are in angstrom. Values in parenthesis are imaginary frequencies.

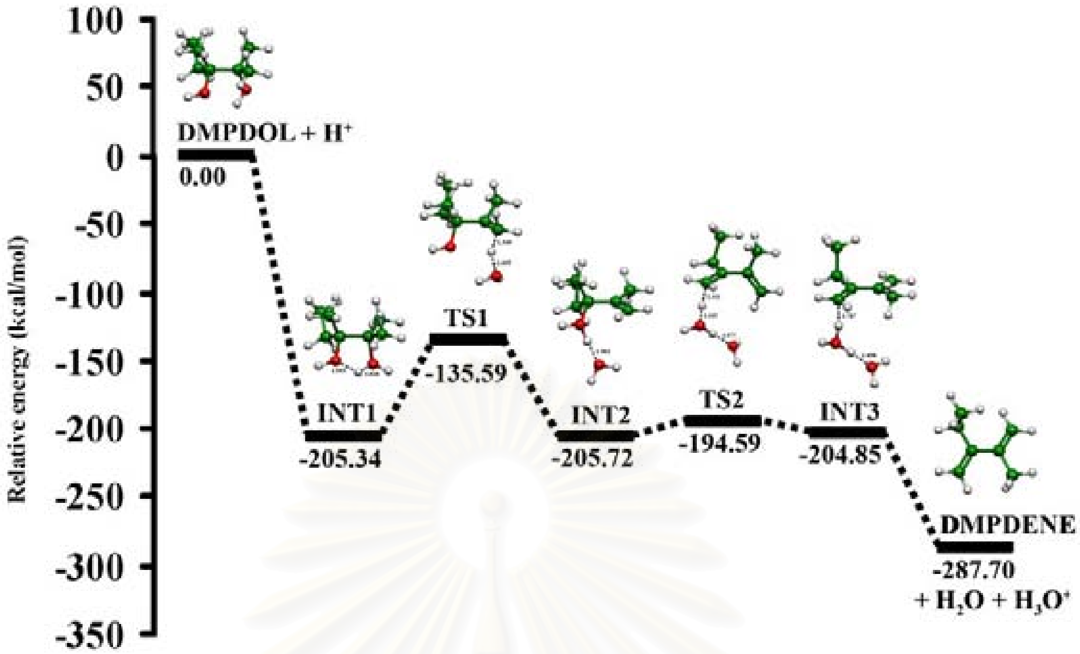

Figure 4.16 Relative energetic profile of conversion reaction of 2,3-dimethyl-2,3-pentanediol (DMPDOL). All energies are based upon B3LYP/6-311+G(d,p) total energies of DMPDOL.

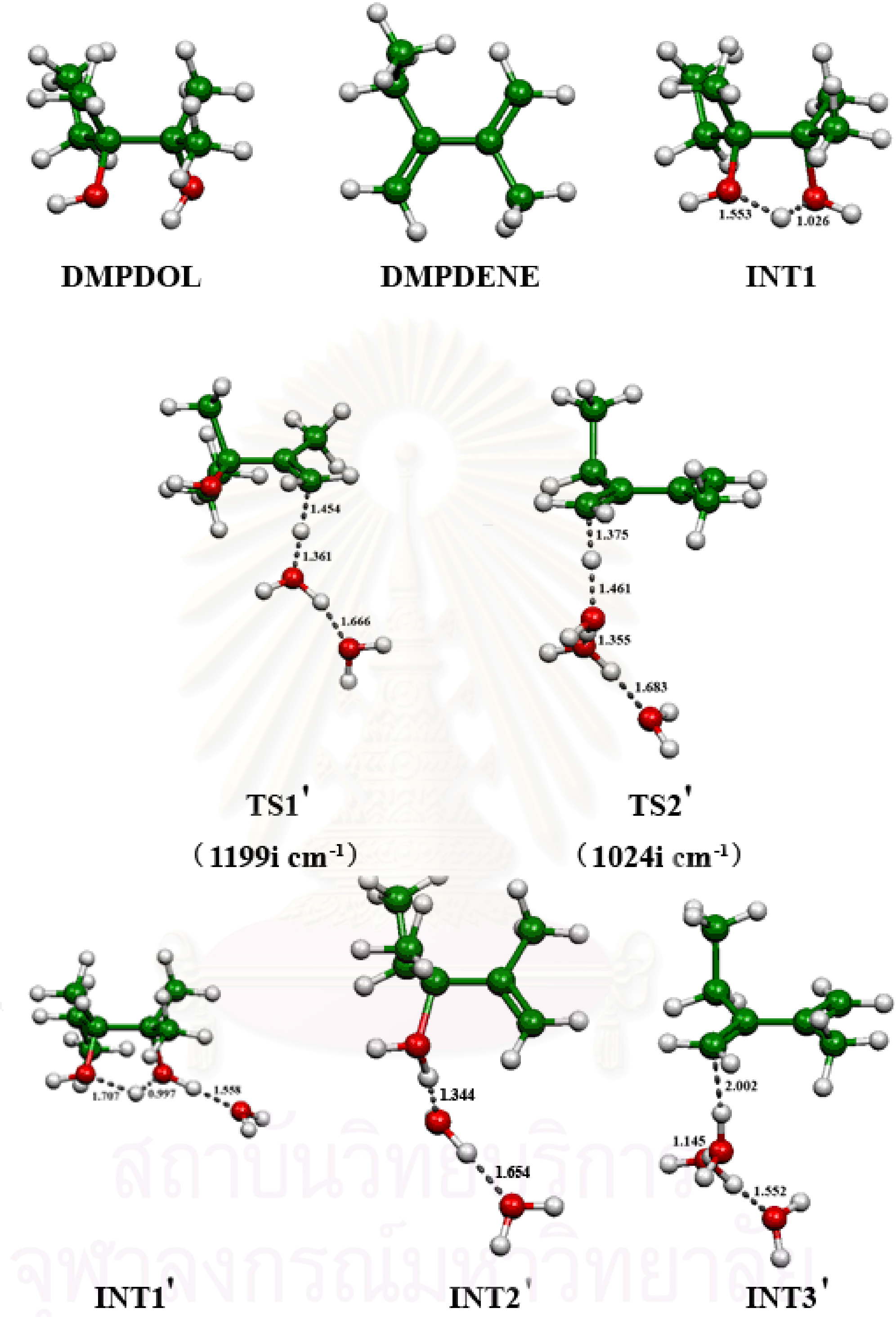

Figure 4.17 The B3LYP/6-311+G(d,p) optimized geometries of conversion reaction of 2,3-dimethyl-2,3-pentanediol, 2,3-dimethyl-1,3-pentadiene, intermediates and transition states in system with a water molecule. Hydrogen bond distances are in angstrom. Values in parenthesis are imaginary frequencies.

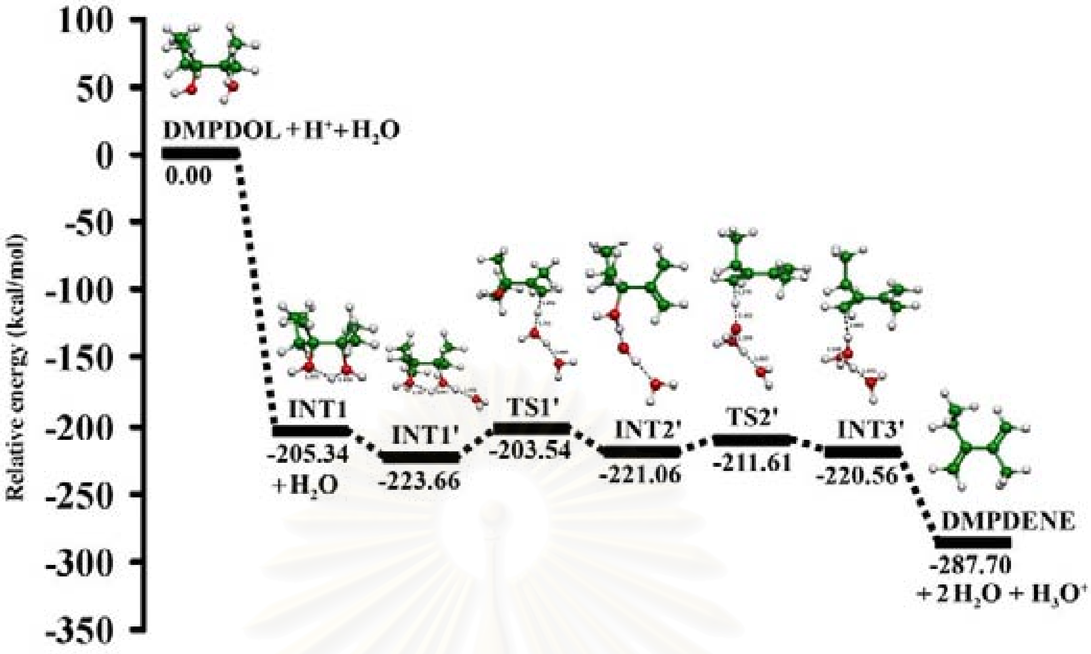

Figure 4.18 Relative energetic profile of conversion reaction of 2,3-dimethyl-2,3-pentanediol (DMPDOL) in system with a water molecule. All energies are based upon B3LYP/6-311+G(d,p) total energies of DMPDOL.

4.3 Comparison of Their Activation Energies

The overall activation thermodynamic quantities and forward rate constants of conversion reaction of 2,3-dimethyl-2,3-butanediol (DMBDOL) to 2,3-dimethyl-1,3-butadiene (DMBDENE) and 2,3-dimethyl-2,3-pentanediol (DMPDOL) to 2,3-dimethyl-1,3-pentadiene (DMPDENE) are shown in Tables 4.9, 4.10 respectively. As a result, addition of water molecule into 2,3-dimethyl-2,3-butanediol in the conversion reaction is shown the lower activation energy than the conversion reaction of 2,3-dimethyl-2,3-butanediol due to the water molecule is sufficient to affect protonation that it can act as a base to remove the adjacent protons from intermediates.

In case of the activation energy of the conversion reaction of 2,3-dimethyl-2,3-pentanediol is higher than the conversion reaction of 2,3-dimethyl-2,3-pentanediol with molecule of water due to the water molecule act as the same way.

The activation energy of the conversion reaction of 2,3-dimethyl-2,3-butanediol and 2,3-dimethyl-2,3-pentanediol are comparatively close to the B3LYP/6-31G(d) and B3LYP/6-311+G(d,p) method. The results show that the activation energy of the conversion reaction of 2,3-dimethyl-2,3-pentanediol is higher than 2,3-dimethyl-2,3-butanediol. As a result, the conversion reaction of 2,3-dimethyl-2,3-pentanediol is hard to convert to 2,3-dimethyl-1,3-pentadiene than the conversion reaction of 2,3-dimethyl-2,3-butanediol to convert to 2,3-dimethyl-1,3-butadiene. Because of the steric energy in the reactant 2,3-dimethyl-2,3-pentanediol is higher than 2,3-dimethyl-2,3-butanediol.

Table 4.9 Activation thermodynamic quantities and rate constants of conversion reaction of 2,3-dimethyl-2,3-butanediol (DMBDOL) conversion, computed at B3LYP/6-311+G(d,p) and B3LYP/6-31G(d) level of theory (in parenthesis).

Reactions /systems	$\Delta^{\ddagger}E$ [a]	$\Delta^{\ddagger}G^{o}_{298}$ [a]	$\Delta^{\ddagger}H^{o}_{298}$ [a]	k_{298} [b]
DMBDOL				
Acid catalyst				
INT1 → TS1	55.13(60.17)	54.61(58.16)	55.07(60.69)	5.72 X 10^{-28}(1.43 X 10^{-30})
INT2 → TS2	8.64(13.21)	8.66(12.07)	8.27(13.38)	2.77 X 10^{6}(8.85 X 10^{3})
Acid catalyst + H_2O				
INT1′ → TS1′	26.21(30.42)	25.23(30.02)	26.05(30.11)	1.97 X 10^{-6}(6.12 X 10^{-10})
INT2′ → TS2′	7.95(12.21)	8.25(8.26)	7.58(13.58)	5.54 X 10^{6}(5.49 X 10^{-6})

[a] In kcal mol^{-1}, [b] Forward (k^{f}) rate constant.

Table 4.10 Activation thermodynamic quantities and rate constants of conversion reaction of 2,3-dimethyl-2,3-pentanediol (DMPDOL) conversion, computed at B3LYP/6-311+G(d,p) and B3LYP/6-31G(d) level of theory (in parenthesis).

Reactions /systems	$\Delta^{\ddagger}E$ [a]	$\Delta^{\ddagger}G^{o}_{298}$ [a]	$\Delta^{\ddagger}H^{o}_{298}$ [a]	k_{298} [b]
DMPDOL				
Acid catalyst				
INT1 → TS1	69.74(67.15)	70.81(67.51)	68.45(66.98)	7.68 X 10^{-40}(2.03 X $10^{-37)}$
INT2 → TS2	11.13(14.66)	12.85(14.15)	9.77(14.87)	2.36 X 10^{3}(2.64 X 10^{2})
Acid catalyst + H_2O				
INT1′ → TS1′	20.12(29.05)	20.00(27.36)	19.68(29.40)	1.36 X 10^{-2}(5.44 X 10^{-8})
INT2′ → TS2′	9.45(19.20)	7.27(18.46)	9.79(18.73)	2.93 X 10^{7}(1.82 X 10^{-1})

[a] In kcal mol^{-1}, [b] Forward (k^{f}) rate constant

CHAPTER V

CONCLUSIONS AND SUGGESTIONS

Conversions of 2,3-dimethyl-2,3-butanediol (DMBDOL) to 2,3-dimethyl-1,3-butadiene (DMBDENE) and 2,3-dimethyl-2,3-pentanediol (DMPDOL) to 2,3-dimethyl-1,3-pentadiene (DMPDENE) have been theoretically studied using DFT method at B3LYP/6-31G(d) and B3LYP/6-311+G(d,p) level of theory. The relative energies of all involved species and the vibrational frequencies of transition states in the rearrangement reaction and their thermodynamic quantities are obtained.

5.1 Conversion of 2,3-dimethyl-2,3-butanediol.

Conversion reaction mechanism of 2,3-dimethyl-2,3-butanediol (DMBDOL) to 2,3-dimethyl-1,3-butadiene (DMBDENE) in acid-catalyzed system is investigated using the DFT method at B3LYP/6-31G(d) and B3LYP/6-311+G(d,p) level of theory. The zero point energies and thermodynamic quantities of activation steps are obtained. The activation energy of conversion reaction of 2,3-dimethyl-2,3-butanediol (DMBDOL) in acid catalyst is 55.13(60.17) kcal/mol (method B3LYP/6-31G(d) is in the parenthesis) and activation energy of conversion reaction of 2,3-dimethyl-2,3-butanediol with molecule of water in acid catalyst (DMBDOL + H_2O) is 26.21(30.42) kcal/mol (method B3LYP/6-31G(d) is in the parenthesis).

5.2 Conversion of 2,3-dimethyl-2,3-butanediol.

Conversion reaction mechanism of 2,3-dimethyl-2,3-pentanediol (DMPDOL) to 2,3-dimethyl-1,3-pentadiene (DMPDENE) in acid catalyzed is investigated using the DFT method at B3LYP/6-31G(d) and B3LYP/6-311+G(d,p) level of theory. The zero point energies and thermodynamic quantities of activation steps are obtained. The activation energy of conversion reaction of 2,3-dimethyl-2,3-pentanediol (DMPDOL) in acid catalyst is 69.74(67.15) kcal/mol (method B3LYP/6-31G(d) is in the parenthesis) and activation energy of conversion reaction of 2,3-dimethyl-2,3-

pentanediol with molecule of water in acid catalyst (DMPDOL + H_2O) is 20.12(29.05) kcal/mol (method B3LYP/6-31G(d) is in the parenthesis).

In conclusion, this study demonstrates the alternative reaction paths by the conversion of diols to diene derivatives from the pinacol rearrangement reaction: addition of water molecule into 2,3-dimethyl-2,3-butanediol in the conversion reaction is shown the lower activation energy than the conversion reaction of 2,3-dimethyl-2,3-butanediol due to the water molecule is sufficient to affect protonation that it can act as a base to remove the adjacent protons from intermediates.

In case of the activation energy of the conversion reaction of 2,3-dimethyl-2,3-pentanediol is higher than the conversion reaction of 2,3-dimethyl-2,3-pentanediol with molecule of water due to the water molecule act as the same way.

Suggestions for further work:

The pinacol rearrangement reaction has preferred 1,2-migration pathway but it also has alternative route to make products as well. Therefore, the steric effect of the reactants should be studied by using other larger structures such as 2,3-dimethyl-2,3-heptanediol. Moreover, the addition of hydrogen halides (chloride or bromide) in the pinacol rearrangement reaction can form diene derivatives such as 1-halo-2,3-dimethyl-2-butene or 3-halo-2,3-dimethyl-1-butene.

The high level of theory such as the MP2/6-311+G(d,p) calculation should improve the geometrical and energetically optimization of relevant systems.

REFERENCES

[1] Chen, Y.; Medforth, C. J.; Smith, K. M.; Alderfer, J.; Dougherty, T. J.; Pandey, R. K.; Effect of meso-substituents on the osmium tetraoxide reaction and pinacol-pinacolone rearrangement of the corresponding vic-drihydroxyporphyrins. *J. Org. Chem.* 66(2001): 3930-3939.

[2] Kong, J.; Mayer, P. S.; Morton, T. H. J. Carbocation rearrangements of trimethylsilyl adducts of saturated acyclic C5-C7 ketones in the gas phase. *J. Mass spectrom.* 217(2002): 257-271.

[3] Collado, I. G.; Hanson, J. R.; Hernandez-Galan, R. Hitchcock, P. Macias-Sanchez, A. Racero, J. C. Novel methoxyl and hydroxyl directed pinacol rearrangements of an isocaryolane sesquiterpenoid under mitsunobu conditions. *Tetrahedron Lett.* 40(1999): 6497-6498.

[4] Nakamura, K.; Osamura, Y. Theoretical study on the migratory aptitude in pinacol rearrangement. *Tetrahedron Lett.* 31 (1990): 251.

[5] Nakamura, K.; Osamura, Y. Theoretical study of the reaction mechanism and migratory aptitude of the pinacol rearrangement., *J. Am. Chem. Soc.* 115 (1993): 9112-9120.

[6] Lezaeta, M. D.; Sattar, W.; Svoronos, P.; Karimia, S.; Subramaniamb, G. Effect of various acids at different concentrations on the pinacol rearrangement. *Tetrahedron Lett.* 43 (2002): 9307- 9309.

[7] Bezouhanova, C.P.; Jabur, F.A.; Zeolite catalysts for pinacol rearrangement. *J. Mol. Catal.* 87 (1994): 39-46.

[8] Bucsi, I.; Molnár, A.; Bartók, M.; Olah, G.A. Transformation of 1, 2-diols over perfluorinated resinsulfonic acids (Nafion-H). *Tetrahedron* 50 (1994): 8195-8202.

[9] Campelo, J. M.; R.; Chakraborty, Marinas, J. M.; Romero, A. A. Gas-phase pinacol conversion on $AlPO_4$, Al_2O_3 and SiO_2 catalysts. *Catal. Lett.* 54 (1998): 91-93.

[10] Török, B.; Bucsi, I.; Beregszászi, T.; Kapocsi, I.; Molnár, Á. Transformation of diols in the presence of heteropoly acids under homogeneous and heterogeneous conditions. *J. Mol. Catal. A* 107 (1996): 305-311.

[11] Ranjbar, P. R.; Kianmehr, E. Facile and fast pinacol rearrangement by $AlCl_3$ in the solid state. *Molecules* 6 (2001): 442-447.

[12] Prasad, K.; Loeser, E.; Chen, G-P.; He, T.; Repic, O. Mechanism of the pinacol–pinacolone rearrangement of 2,3-di-(3-pyridyl)-2,3-butanediol in sulfuric acid. *Tetrahedron Lett.* 43 (2002): 2161-2165.

[13] Adam, W.; Bach, R.D; Dmitrenko, O.; Saha-Möller, C.R. A computational study of the hydroxy-group directivity in the peroxyformic scid epoxidation of the chiral allylic alcohol (*Z*)-3-methyl-3-penten-2-ol: control of threo diastereoselectivity through allylic strain and hydrogen bonding. *J. Org. Chem.* 65 (2000): 6715-6728.

[14] Fry, J. A.; Grant, A. A.; Allukian, M. Pinacol reduction-cum-rearrangement. A re-examination of the reaction of aryl alkyl ketones by zinc-aluminum chloride. *Tetrahedron Lett.* 43(2002): 4391-4393.

[15] Gazquez, L. J.; Cedillo, A.; Gomez, B.; Vela, A. Molecular Fragments in Density Functional Theory. *J. Phys. Chem. A* 110(2006): 4535-4537.

[16] Neurock, M.; Janik, J. M.; Davis, J. R. A density functional theory study of the alkylation of isobutene with butene over phosphotungstic acid. *J. of catalysis.* 244(2006): 65-77.

[17] Ge, M.; Wang, W.; Wang, D. A density functional study on iodine-water complexes. *Chemical Physics.* 328(2006): 165-172.

[18] Marder, B. T.; Zhao, H.; Lin, Z. Density functional theory studies on the mechanism of the reduction of CO_2 to CO catalyzed by Copper(I) Boryl complexes. *J. Am. Chem. Soc.* 128(2006): 15637-15643.

[19] Petris, G. de.; Giacomello, P.; Pizzabiocca, A.; Renzi, G.; Speranza, M. Stereochemical effect in the gas-phase pinacol rearrangement. 2. ring contraction versus methyl migration in cis- and trans-1,2-dimethylcyclohexane-1,2-diol. *J Am Chem Soc.* 110 (1988): 1098-1103.

[20] Svoronos, P.; Lazaeta, M. D.; Sattar, W.; Karimi, S.; Subramanium, G. Effect of various acids at different concentrations on the pinacol rearrangement. *Tetrahedron Letters.* 43(2002): 9307-9309.

[21] Hsien, M.; Sheu, H.-T.; Lee, T.; Cheng, S.; Lee, J.-F. Fe-substituted molecular sieves as catalysts in liquid phase pinacol rearrangement. *J. Mol. Catal. A* 181 (2002): 189-200.

[22] Kita, Y.; Yoshida, Y.; Mihara, S.; Furukawa, A.; Higuchi, K.; Fang, D.; Fujioka, H. Efficient pinacol rearrangement mediated by trimethyl orthoformate. *Tetrahedron Lett*. 38(1997): 8315-8318.

[23] Kita, Y.; Yoshida, Y.; Mihara, S.; Furukawa, A.; Higuchi, K.; Fang, D-F.; Fujioka, H. Non-dehydrative pinacol rearrangement using a Lewis acid-trialkyl orthoester combined system. *Tetrahedron* 54 (1998): 14689-14704.

[24] Ikushima, Y.; Hatakeda, K.; Sato, O.; Yokoyama, T.; Arai, M. Accelerration of synthetic organic reactions using supercritical water: noncatalytic Beckmann and pinacol rearrangement. *J. Am. Chem. Soc* 122(2000): 1908-1918.

[25] Hsu, B. Y.; Cheng. S. Pinacol rearrangement over metal-substituted aluminophosphate molecular sieves. *Microporous and Mesoporous Mater*. 21 (1998): 5005-5015.

[26] Smith, B. W. Ethylene glycol to acetaldehyde-dehydration or a concerted mechanism. *Tetrahedron* 58 (2002): 2091-2094.

[27] Dai, Z.; Hatano, B.; Tagaya, H. Catalytic dehydration of propylene glycol with salts in near-critical water. *App. Catal. A* 258 (2004): 189-193.

[28] Pachuau, Z.; Lyngdoh, D. R. Molecular orbital studies on the Wagner-Meerwein migration in some acyclic pinacol–pinacolone rearrangements. *J. Chem. Sci*. 116 (2004): 83-91.

[29] Rungnim, C.; Ruangpornvisuti, V. A density functional study of propylene glycol conversion to propanal and propanone of various acid-catalyzed reaction models: a water-addition effect. *J. Comp. Chem.* 26 (2005): 1592-1599.

[30] Lewars, E. Computational chemistry: Introduction to the theory and applications of molecular and quantum mechanics Trent University Peterborough, Ontario (2003).

[31] Atkins, P. W. Quanta 2nd ed. Oxford University (1991).

[32] Becke, A. D. Density-functional exchange-energy approximation with correct asymptotic behavior *Phys. Rev. A* 38 (1988): 3098.

[33] Lee, C.; Yang, W.; Parr, R. G. Development of the Colle-Salvetti correlation-energy formula into a functional of the electron density *Phys. Rev.* B 37 (1988): 785.

[34] Hammond, S. G. A Correlation of Reaction Rates. *J. Am. Chem. Soc*. 77 (1955): 334-338.

[35] Donahue, M. N. Revisiting the Hammond postulate: the role of reactant and product ionic states in regulating barrier heights, locations, and transition state frequencies. *J. Phys. Chem. A* 105 (2001): 1489-1497.

[36] Frisch, M. J.; Trucks, G. W.; Schlegel, H. B.; Scuseria, G. E.; Robb, M. A.; Cheeseman, J. R.; Montgomery, J. A.; Vreven, T.; Kudin, K.N.; Burant, J. C.; Millam, J. M.; Iyengar, S. S.; Tomasi, J.; Barone, V.; Mennucci, B.; Cossi, M.; Scalmani, G.; Rega, N.; Petersson, G. A.; Nakatsuji, H.; Hada, M.; Ehara, M.; Toyota, K.; Fukuda, R.; Hasegawa, J.; Ishida, M.; Nakajima, T.; Honda, Y.; Kitao, O.; Nakai, H.; Klene, M.; Li, X.; Knox, J. E.; Hratchian, H. P.; Cross, J. B.; Adamo, C.; Jaramillo, J.; Gomperts, R.; Stratmann, R. E.; Yazyev, O.; Austin, J.; Cammi, R.; Pomelli, C.; Ochterski, J. W.; Ayala, P. Y.; Morokuma, K.; Voth, G. A.; Salvador, P.; Dannenberg, J. J.; Zakrzewski, V. G.; Dapprich, S.; Daniels, A. D.; Strain, M. C.; Farkas, O.; Malick, D. K.; Rabuck, A. D.; Raghavachari, K.; Foresman, J. B.; Ortiz, J. V.; Cui, Q.; Baboul, A. G.; Clifford, S.; Cioslowski, J.; Stefanov, B. B.; Liu, G.; Liashenko, A.; Piskorz, P.; Komaromi, I.; Martin, R. L.; Fox, D. J.; Keith, T.; Al-Laham, M. A.; Peng, C. Y.; Nanayakkara, A.; Challacombe, M.; Gill, P. M. W.; Johnson, B.; Chen, W.; Wong, M. W.; Gonzalez, C.; Pople, J. A.; Gaussian 03, Revision B.03, Gaussian, Inc., Pittsburgh PA, 2003.

[37] Schaftenaar, G.; MOLDEN 3.7, CAOS/CAMM Center, Nijmegen Toernooiveld, Nijmegen, Netherlands, 1991.

[38] Flükiger, P.; Lüthi, H. P.; Portmann, S.; Weber, J.; MOLEKEL 4.3: Swiss Center for Scientific Computing, Manno (Switzerland), 2000.

[39] Suzuki, K.; Shinohara, T. Pinacol rearrangement for constructing asymmetric centers adjacent to heterocycles. *Tetrahedron Lett.* 43(2002): 6937-6940.

[40] Navarro-Vazquez, A.; Rodriguez, M.D.; Martinez-Esperon, F.; Garcia, A.; Saa, C.; Dominguez, D. Acid-catalyzed cyclization of acyliminium ions derived from allenamides. A new entry to protoberberines. *Tetrahedron Lett.* 48(2007): 2741-2743

[41] Hoang, M.; Gadosy, T.; Ghasi, H.; Hou, F.; Hopkinson A. C.; Johnston L. J.; Lee-Ruff E. Photochemical pinacol rearrangement. *J. Org. Chem.* 63(1998): 7168-7171.

[42] Johnson, L. J.; Lee-ruff, E.; Mladenova, G.; Singh, G.; Acton, A.; Chen, L.; Rinco, O. Photochemical pinacol rearrangements of unsymmetrical diols. *J. Org. Chem.* 69(2004), 2017-2023.

[43] Marson, C. M.; Oare, C. A.; Mcgregor, J.; Walsgrove, T.; Grinter, T. J. A sequential stereocontrolled cyclopropane ring formation and semi-pinacol rearrangement. *Tetrahedron Lett.* 44(2003), 141-143.

[44] Maffei, M.; Buono, G. A two step synthesis of 2-oxo-2-vinyl 1,3,2-dioxaphospholanes and –dioxaphosphorinanes. *Tetrahedron* 59(2003), 8821-8825.

[45] Crimmins, M.; Carolls, C. A.; Wells, A. J. Pinacol-type rearrangements of intramolecular photocycloadducts: application of the 2,2-dimethyl-4-pentenoate protecting group. *Tetrahedron Lett.* 39(1998), 7005-7008.

[46] Bach, T.; Eilers, F. Pinacol-type rearrangements reactions of 2-phenyl-3-silyloxyoxetanes: The influence of the lewis acid on the regioselectivity. *J. Org. Chem.* 64(1999), 8041-8044.

[47] Manning, A. R.; Mcglinchey, M. J.; Ortin, Y.; Grealis, J.; Scully, C.; Muller-bunz, H. McMurray reaction of (η^5-acetylcyclopentadienyl) cobalt-(η^4-tetraphenylcyclobutadiene) with benzophenone: ketones coupling and a pinacol/pinacolone rearrangement. *J. of Organometallic Chemistry* 689(2004), 4683-4690.

[48] Lontsi, D.; Tapondju, L. A.; Ngounou, F. N.; Sondengam, B. L.; Connolly, J. D. Reactions of 2,3,19-trihydroxyurs-12-triterpenoids: pinacol

rearrangement of methyl 2α,3β,19α-trihydroxyurs-12-en-28-oate. *Tertrahedron* 54(1998), 2099-2106.

[49] Panov, A. G.; Fripiat, J. J.; Acetone condensation reaction on acid catalysts *J. Catal.* 178 (1998), 188-197.

[50] Sawaki, Y.; Kimura, M.; Kobayashi, K.; Yamamoto, Y. Electrooxidative pinacol-type rearrangement of β-hydroxy sulfides. Efficient C-S cleavage mediated by chloride ion oxidation. *Tetrahedron.* 52(1996), 4303-4310.

[51] Török, B.; Bucsi, I.; Beregszászi, T.; Kapocsi, I.; Molnár, Á. Transformation of diols in the presence of heteropoly acids under homogeneous and heterogeneous conditions. *J. Mol. Catal. A* 107 (1996): 305-311.

[52] Ranjbar, P. R.; Kianmehr, E. Facile and fast pinacol rearrangement by $AlCl_3$ in the solid state. *Molecules* 6 (2001): 442-447.

[53] Prasad, K.; Loeser, E.; Chen, G-P.; He, T.; Repic, O. Mechanism of the pinacol–pinacolone rearrangement of 2,3-di-(3-pyridyl)-2,3-butanediol in sulfuric acid. *Tetrahedron Lett.* 43 (2002): 2161-2165.

APPENDIX A

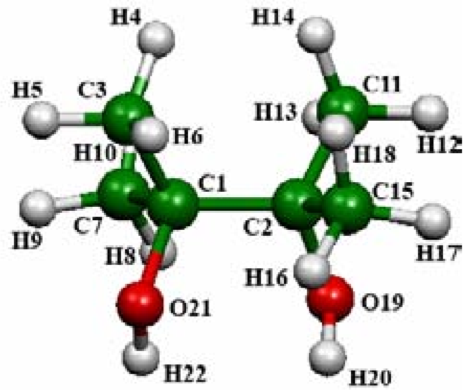

Table 1 Geometrical parameters of 2,3-dimethyl-2,3-butanediol.

Bond Length	Value (Angstroms)	Angle	Value (Degrees)	Dihedral	Value (Degrees)
R(1,2)	1.5755	A(1,2,11)	113.1062	D(1,2,11,12)	176.1044
R(1,3)	1.5300	A(1,2,15)	111.6735	D(1,2,11,13)	-65.1755
R(1,7)	1.5366	A(1,2,19)	107.5948	D(1,2,11,14)	56.3668
R(1,21)	1.4462	A(1,3,4)	111.5882	D(1,2,15,16)	50.0577
R(2,11)	1.5300	A(1,3,5)	109.4004	D(1,2,15,17)	170.0719
R(2,15)	1.5377	A(1,3,6)	111.0074	D(1,2,15,18)	-70.7274
R(2,19)	1.4458	A(1,7,8)	110.9634	D(1,2,19,20)	-80.2507
R(3,4)	1.0922	A(1,7,9)	109.1180	D(2,1,3,4)	56.3244
R(3,5)	1.0922	A(1,7,10)	111.8091	D(2,1,3,5)	176.0754
R(3,6)	1.0906	A(1,21,22)	107.7510	D(2,1,3,6)	-65.2040
R(7,8)	1.0930	A(2,1,3)	113.1015	D(2,1,7,8)	50.0244
R(7,9)	1.0928	A(2,1,7)	111.6944	D(2,1,7,9)	170.0775
R(7,10)	1.0920	A(2,1,21)	107.5509	D(2,1,7,10)	-70.7407
R(11,12)	1.0905	A(2,11,12)	109.3914	D(2,1,21,22)	-81.4488
R(11,13)	1.0922	A(2,11,13)	111.0160	D(3,1,2,11)	-74.2603
R(11,14)	1.0922	A(2,11,14)	111.5866	D(3,1,2,15)	51.0279
R(15,16)	1.0930	A(2,15,16)	110.9614	D(3,1,2,19)	170.2602
R(15,17)	1.0927	A(2,15,17)	109.0955	D(3,1,7,8)	176.8037
R(15,18)	1.0920	A(2,15,18)	111.8217	D(3,1,7,9)	-63.1431
R(19,20)	0.9631	A(2,19,20)	107.6829	D(3,1,7,10)	56.0385
R(21,22)	0.9630			D(3,1,21,22)	157.8382
				D(7,1,2,11)	51.0495
				D(7,1,2,15)	176.3378
				D(7,1,2,19)	-64.4299
				D(7,1,3,4)	-69.6677
				D(7,1,3,5)	50.0831
				D(7,1,3,6)	168.8036
				D(7,1,21,22)	39.6568
				D(19,2,11,12)	-66.8687
				D(19,2,11,13)	51.8512
				D(19,2,11,14)	173.3936
				D(19,2,15,16)	-68.5054
				D(19,2,15,17)	51.5087
				D(19,2,15,18)	170.7093
				D(19,2,1,21)	54.7974
				D(21,1,3,4)	173.3027
				D(21,1,3,5)	-66.9463
				D(21,1,3,6)	51.7741
				D(21,1,7,8)	-68.5028
				D(21,1,7,9)	51.5503
				D(21,1,7,10)	170.7320

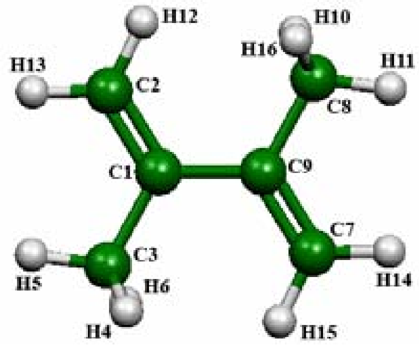

Table 2 Geometrical parameters of 2,3-dimethyl-1,3-butadiene.

Bond Length	Value (Angstroms)	Angle	Value (Degrees)	Dihedral	Value (Degrees)
R(1,2)	1.3427	A(1,2,12)	122.7262	D(1,9,7,14)	179.9965
R(1,3)	1.5114	A(1,2,13)	120.9432	D(1,9,7,15)	0.0000
R(1,9)	1.4821	A(1,3,4)	111.3969	D(1,9,8,10)	-59.8552
R(2,12)	1.0822	A(1,3,5)	110.6321	D(1,9,8,11)	179.9737
R(2,13)	1.0841	A(1,3,6)	111.3964	D(1,9,8,16)	59.8013
R(3,4)	1.0943	A(1,9,7)	121.6334	D(2,1,3,4)	-120.2378
R(3,5)	1.0908	A(1,9,8)	118.5049	D(2,1,3,5)	-0.0642
R(3,6)	1.0944	A(2,1,3)	119.8619	D(2,1,3,6)	120.1075
R(7,9)	1.3427	A(2,1,9)	121.6354	D(2,1,9,7)	-179.9543
R(7,14)	1.0841	A(3,1,9)	118.5025	D(2,1,9,8)	0.0401
R(7,15)	1.0822	A(7,9,8)	119.8615	D(3,1,2,12)	-179.9956
R(8,9)	1.5114	A(9,7,14)	120.9437	D(3,1,2,13)	0.0029
R(8,10)	1.0943	A(9,7,15)	122.7256	D(3,1,9,7)	0.0426
R(8,11)	1.0908	A(9,8,10)	111.3963	D(3,1,9,8)	-179.9628
R(8,16)	1.0943	A(9,8,11)	110.6340	D(4,3,1,9)	59.7650
		A(9,8,16)	111.3954	D(5,3,1,9)	179.9385
				D(6,3,1,9)	-59.8895
				D(7,9,8,10)	120.1394
				D(7,9,8,11)	-0.0316
				D(7,9,8,16)	-120.2040
				D(8,9,7,14)	0.0000
				D(8,9,7,15)	-179.9969

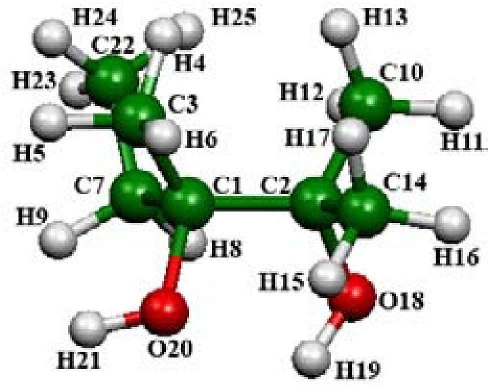

Table 3 Geometrical parameters of 2,3-dimethyl-2,3-pentanediol.

Bond Length	Value (Angstroms)	Angle	Value (Degrees)	Dihedral	Value (Degrees)
R(1,2)	1.5762	A(1,2,10)	113.9669	D(1,2,10,11)	177.3778
R(1,3)	1.5324	A(1,2,14)	111.2969	D(1,2,10,12)	-64.5112
R(1,7)	1.5515	A(1,2,18)	107.7616	D(1,2,10,13)	58.0589
R(1,20)	1.4554	A(1,3,4)	112.2052	D(1,2,14,15)	50.8607
R(2,10)	1.5293	A(1,3,5)	110.0016	D(1,2,14,16)	170.0877
R(2,14)	1.5393	A(1,3,6)	110.5041	D(1,2,14,17)	-70.7551
R(2,18)	1.4351	A(1,7,8)	108.0307	D(1,2,18,19)	-48.8847
R(3,4)	1.0922	A(1,7,9)	106.6269	D(1,7,22,23)	178.8625
R(3,5)	1.0948	A(1,7,22)	118.0124	D(1,7,22,24)	-62.3723
R(3,6)	1.0897	A(1,20,21)	108.8341	D(1,7,22,25)	59.3761
R(7,8)	1.0924	A(2,1,3)	113.4233	D(2,1,3,4)	59.0339
R(7,9)	1.0985	A(2,1,7)	113.0576	D(2,1,3,5)	178.6682
R(7,22)	1.5354	A(2,1,20)	101.8764	D(2,1,3,6)	-62.4696
R(10,11)	1.0923	A(2,10,11)	108.6605	D(2,1,7,8)	36.0050
R(10,12)	1.0898	A(2,10,12)	111.1323	D(2,1,7,9)	149.5912
R(10,13)	1.0920	A(2,10,13)	112.0062	D(2,1,7,22)	-90.0627
R(14,15)	1.0913	A(2,14,15)	111.1719	D(2,1,20,21)	-164.9059
R(14,16)	1.0919	A(2,14,16)	108.3421	D(3,1,2,10)	-73.3502
R(14,17)	1.0929	A(2,14,17)	112.0304	D(3,1,2,14)	51.3121
R(18,19)	0.9663	A(2,18,19)	106.2339	D(3,1,2,18)	170.5235
R(20,21)	0.9621	A(3,1,7)	111.8447	D(3,1,7,8)	165.5064
R(22,23)	1.0935	A(3,1,20)	108.2036	D(3,1,7,9)	-80.9073
R(22,24)	1.0927	A(7,1,20)	107.6826	D(3,1,7,22)	39.4386
R(22,25)	1.0904	A(7,22,23)	109.5109	D(4,3,1,7)	-70.2763
		A(7,22,24)	111.9001	D(4,3,1,20)	171.2788
		A(7,22,25)	112.8393	D(5,3,1,7)	49.3579
		A(8,7,9)	106.0217	D(5,3,1,20)	-69.0868
		A(8,7,22)	110.4181	D(6,3,1,7)	168.2200
		A(9,7,22)	107.0372	D(6,3,1,20)	49.7753
		A(10,2,14)	109.6745	D(7,1,2,10)	55.3410
		A(10,2,18)	105.0276	D(7,1,2,14)	-179.9965
		A(11,10,12)	107.5198	D(7,1,2,18)	-60.7851
		A(11,10,13)	108.0734	D(8,7,1,20)	-75.7393
		A(14,2,18)	108.7981	D(8,7,22,23)	53.9627
		A(15,14,16)	108.5736	D(8,7,22,24)	172.7278
		A(15,14,17)	108.5221	D(8,7,22,25)	-65.5236
		A(23,22,24)	107.2343	D(9,7,1,20)	37.8469
		A(23,22,25)	107.3340	D(9,7,22,23)	-61.0044
				D(9,7,22,24)	57.7607
				D(9,7,22,25)	179.5091
				D(10,2,1,20)	170.6092

Bond Length	Value (Angstroms)	Angle	Value (Degrees)	Dihedral	Value (Degrees)
				D(10,2,14,15)	177.9023
				D(10,2,14,16)	-62.8707
				D(10,2,14,17)	56.2864
				D(10,2,18,19)	-170.7310
				D(11,10,2,14)	51.8527
				D(11,10,2,18)	-64.9115
				D(12,10,2,14)	169.9636
				D(12,10,2,18)	53.1993
				D(13,10,2,14)	-67.4661
				D(13,10,2,18)	175.7696
				D(14,2,1,20)	-64.7283
				D(14,2,18,19)	71.9061
				D(15,14,2,18)	-67.7305
				D(16,14,2,18)	51.4964
				D(17,14,2,18)	170.6536
				D(18,2,1,20)	54.4830
				D(20,1,7,22)	158.1929

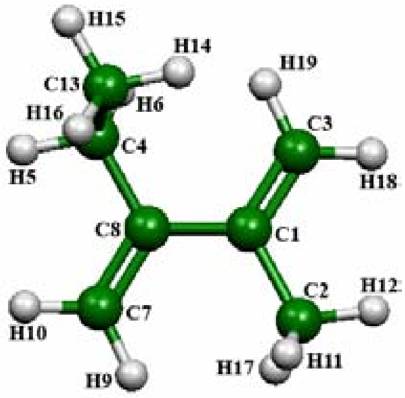

Table 4 Geometrical parameters of 2,3-dimethyl-1,3-butadiene.

Bond Length	Value (Angstroms)	Angle	Value (Degrees)	Dihedral	Value (Degrees)
R(1,2)	1.5130	A(1,2,11)	111.9779	D(1,8,4,5)	162.4349
R(1,3)	1.3428	A(1,2,12)	110.6429	D(1,8,4,6)	46.9330
R(1,8)	1.4802	A(1,2,17)	111.0086	D(1,8,4,13)	-76.3892
R(2,11)	1.0937	A(1,3,18)	120.8089	D(1,8,7,9)	0.8323
R(2,12)	1.0919	A(1,3,19)	123.0729	D(1,8,7,10)	-178.9733
R(2,17)	1.0964	A(1,8,4)	119.5062	D(2,1,3,18)	-1.1603
R(3,18)	1.0845	A(1,8,7)	121.2120	D(2,1,3,19)	178.4986
R(3,19)	1.0825	A(2,1,3)	119.4244	D(2,1,8,4)	172.5720
R(4,5)	1.0940	A(2,1,8)	118.1395	D(2,1,8,7)	-6.5924
R(4,6)	1.0948	A(3,1,8)	122.4201	D(3,1,2,11)	123.2079
R(4,8)	1.5190	A(4,8,7)	119.2764	D(3,1,2,12)	
R(4,13)	1.5400	A(4,13,14)	111.6797	D(3,1,2,17)	
R(7,8)	1.3432	A(4,13,15)	110.7296	D(3,1,8,4)	
R(7,9)	1.0829	A(4,13,16)	110.6489	D(3,1,8,7)	
R(7,10)	1.0849	A(5,4,6)	105.9155	D(4,8,7,9)	
R(13,14)	1.0931	A(5,4,8)	108.3263	D(4,8,7,10)	
R(13,15)	1.0948	A(5,4,13)	108.9146	D(5,4,8,7)	
R(13,16)	1.0939	A(6,4,8)	110.3016	D(5,4,13,14)	
		A(6,4,13)	109.4467	D(5,4,13,15)	
		A(8,7,9)	122.9868	D(5,4,13,16)	
		A(8,7,10)	120.8480	D(6,4,8,7)	
		A(11,2,12)	107.9173	D(6,4,13,14)	
		A(11,2,17)	107.2026	D(6,4,13,15)	
		A(12,2,17)	107.9148	D(6,4,13,16)	
		A(14,13,15)	107.9532	D(7,8,4,13)	
		A(14,13,16)	107.7077	D(8,1,2,11)	
		A(15,13,16)	107.9765	D(8,1,2,12)	
		A(18,3,19)	116.1173	D(8,1,2,17)	
				D(8,1,3,18)	
				D(8,1,3,19)	
				D(8,4,13,14)	
				D(8,4,13,15)	
				D(8,4,13,16)	

APPENDIX B

Table 1 Cartesian coordinates of first transition state of 2,3-dimethyl-2,3-butanediol in pinacol rearrangement by B3LYP/6-311^{+}G(d,p) method.

Atomic Type	Coordinate (Angstroms)		
	X	Y	Z
C	-0.80866500	-0.46142500	0.01279300
C	-1.30431600	-0.57204900	1.46593500
H	-1.91204000	0.29126900	1.75859600
H	-1.93779000	-1.46203700	1.54097500
H	-0.47162500	-0.67971000	2.16302300
C	-1.96921800	-0.55252100	-0.98459300
H	-1.62976700	-0.44483000	-2.01998200
H	-2.45345100	-1.53044500	-0.89065800
H	-2.73594300	0.20266100	-0.78752800
C	-0.68102300	2.08264100	-0.47897300
H	0.00612500	2.91289200	-0.66934000
H	-1.38267400	1.99394700	-1.31376800
H	-1.26015200	2.32927500	0.42216300
C	1.20232400	0.94677800	0.75262800
H	1.85283000	1.77519800	0.45446000
O	2.98737200	-0.47185100	-0.34516700
H	2.81376100	-0.27562000	-1.28456900
O	0.13518900	-1.52997400	-0.26736600
H	-0.36114600	-2.35821400	-0.37726400
H	2.72569900	-1.40459100	-0.24223500
C	0.04892000	0.81661800	-0.15461200
H	2.06724300	-0.08290200	0.73281300
H	0.77031000	1.18745800	1.73451100

Table 2 Cartesian coordinates of second transition state of 2,3-dimethyl-2,3-butanediol in pinacol rearrangement by B3LYP/6-311^{+}G(d,p) method.

Atomic Type	Coordinate (Angstroms)		
	X	Y	Z
C	0.88444700	-0.68047500	0.18214400
C	0.39620500	-1.50500900	-0.79523600
H	0.54138100	-1.24336600	-1.84241400
H	0.22271500	-2.55900500	-0.57451300
H	-1.03534400	-1.03733100	-0.71795900
C	0.93934200	-1.09433900	1.62057000
H	0.40553600	-0.37004300	2.24734200
H	0.54634300	-2.09954900	1.78903900
H	1.98230800	-1.06774600	1.96149600
C	2.90153400	0.74657300	-0.37016300
H	3.19441900	1.75824800	-0.65967800
H	3.45055800	0.48169900	0.54138900
H	3.22432700	0.05314800	-1.15496600
C	0.59173300	1.73364500	-0.24797700
O	-2.17341600	-0.85693100	-0.88364800
H	-2.70306900	-1.67093400	-0.82081300
C	1.40397500	0.67776900	-0.15728800
H	-0.48025600	1.67012800	-0.08164300
H	0.98275300	2.71532900	-0.49660500
H	-2.58415300	-0.12472800	-0.31135500
O	-3.22367500	1.05653100	0.51623400
H	-3.29185700	1.06700000	1.48297600
H	-3.98234500	1.56137000	0.18471300

Table 3 Cartesian coordinates of first transition state of 2,3-dimethyl-2,3-butanediol with one molecule of water in pinacol rearrangement by B3LYP/6-311^{+}G(d,p) method.

Atomic Type	Coordinate (Angstroms)		
	X	Y	Z
C	1.55363000	-0.39951300	0.13192000
C	2.93340300	-0.18053600	-0.57050600
H	3.48725700	0.65961400	-0.14345500
H	3.52461000	-1.08925900	-0.41527100
H	2.80525300	-0.03029600	-1.64567100
C	1.74875500	-0.60575600	1.65226400
H	0.78727500	-0.67142200	2.16999200
H	2.28060800	-1.55043200	1.80435100
H	2.34923900	0.18372600	2.10962900
C	0.99048400	2.11452300	0.41702100
H	0.08061500	2.72079100	0.46848500
H	1.48395800	2.07524800	1.38808500
H	1.66316500	2.64827500	-0.27860200
C	-0.21762300	0.67280700	-1.26597600
H	-0.70267700	1.59903100	-1.57267100
O	-2.42317100	-0.90859400	-0.39115800
H	-3.13421400	-0.35750600	0.03164400
O	0.86907000	-1.49990100	-0.44399900
H	1.39670200	-2.30361500	-0.31121500
H	-2.00438600	-1.37242600	0.34865400
C	0.72435500	0.79873400	-0.20262200
H	-1.11055800	-0.25325900	-0.92838600
H	0.23179800	0.13271500	-2.11617500
O	-4.61154000	0.27344200	0.54202800
H	-5.26582700	-0.42123300	0.72142500
H	-4.94571300	0.70892300	-0.25838700

Table 4 Cartesian coordinates of second transition state of 2,3-dimethyl-2,3-butanediol with one molecule of water in pinacol rearrangement by B3LYP/6-311^{+}G(d,p) method.

Atomic Type	Coordinate (Angstroms)		
	X	Y	Z
C	1.52827400	-0.26462400	0.65054000
C	1.46376800	-1.61655100	0.30988800
H	2.05877300	-1.98422300	-0.52461700
H	1.31245400	-2.33291700	1.11746800
H	0.23281000	-1.59636000	-0.27009000
C	0.95223900	0.16631700	1.97119300
H	0.06065700	0.78640700	1.82006900
H	0.67270000	-0.69628200	2.57886300
H	1.67622500	0.76000300	2.53909100
C	2.51788800	0.26578700	-1.66152000
H	2.83750900	1.11940900	-2.26336900
H	3.36953200	-0.41948200	-1.57766000
H	1.72683100	-0.25555500	-2.21315500
C	2.08162400	2.02996800	0.04321700
O	-0.91148300	-1.65113300	-0.88895600
H	-1.18333000	-2.57597400	-1.02391300
C	2.03523100	0.72492500	-0.30363600
H	1.74875900	2.40043500	1.00646400
H	2.47564000	2.77422300	-0.64253200
H	-1.61615600	-1.18320300	-0.30263600
O	-2.49385700	-0.32148300	0.63320100
H	-3.00303700	-0.79921900	1.30659100
H	-3.16251900	0.24549900	0.16552200
H	-4.75513600	1.02380900	-1.43856500
O	-4.49775500	1.08551200	-0.50613200
H	-4.70109200	1.99533100	-0.24052900

Table 5 Cartesian coordinates of first transition state of 2,3-dimethyl-2,3-pentanediol in pinacol rearrangement by B3LYP/6-311^{+}G(d,p) method.

Atomic Type	Coordinate (Angstroms)		
	X	Y	Z
C	-0.40857300	-0.57620900	0.09588600
C	-0.77206300	-0.79089200	1.57619500
H	-1.43317100	-0.00333600	1.95433400
H	-1.31012000	-1.74100200	1.65856300
H	0.12084200	-0.84307000	2.20141100
C	-1.63227800	-0.74229300	-0.81236700
H	-1.38962500	-0.56196600	-1.86472500
H	-2.01239000	-1.76592500	-0.72673000
C	-0.56301300	1.98515300	-0.28617100
H	0.02461400	2.88557500	-0.49029100
H	-1.31844700	1.86024500	-1.06769600
H	-1.08795100	2.13881800	0.66729200
C	1.51316200	0.99305800	0.74303500
H	2.05586800	1.89221600	0.43428400
O	3.32978100	-0.20008800	-0.55325200
H	3.06276700	0.01421400	-1.46643400
O	0.60651200	-1.53533200	-0.30515200
H	0.18367500	-2.40344600	-0.41467700
H	3.16693500	-1.15728400	-0.47369300
C	0.30756300	0.78535400	-0.07779200
H	2.46734900	0.05480200	0.60916000
H	1.14130000	1.15213200	1.76532200
C	-2.78137600	0.19810800	-0.40393200
H	-2.45260300	1.21398900	-0.47316500
H	-3.61490800	0.04764000	-1.05775500
H	-3.07501700	-0.01391200	0.60290600

Table 6 Cartesian coordinates of second transition state of 2,3-dimethyl-2,3-pentanediol in pinacol rearrangement by B3LYP/6-311$^+$G(d,p) method.

Atomic Type	Coordinate (Angstroms)		
	X	Y	Z
C	-0.63333400	-0.42034000	0.27169800
C	0.00413000	-0.97677800	1.34706600
H	0.16261300	-0.38336500	2.24608400
H	0.00500500	-2.06018300	1.47069800
H	1.37220100	-1.10243500	0.90973700
C	-1.09154500	-1.24925500	-0.89145200
H	-0.65618700	-0.86740000	-1.82252700
H	-0.84603400	-2.30673900	-0.77015500
C	-2.25562800	1.47574200	0.74778100
H	-2.33839200	2.56465700	0.73279000
H	-3.06900000	1.06616900	0.13942500
H	-2.41576400	1.12996500	1.77511000
C	0.01832000	1.90623100	-0.23011900
O	2.52915800	-1.04754600	0.78745600
H	2.94082600	-1.91672000	0.64155600
C	-0.89654900	1.05049000	0.23122200
H	0.98836400	1.58899700	-0.60255400
H	-0.17945800	2.97327600	-0.24954100
H	2.86194000	-0.38068500	0.09730100
O	3.40082600	0.69980900	-0.91797500
H	3.22856600	0.68242500	-1.87119300
H	4.26720100	1.11973600	-0.80544000
C	-2.61860300	-1.12500400	-1.06427000
H	-2.88123400	-0.09949900	-1.22688900
H	-2.92929300	-1.70778100	-1.90865600
H	-3.11197800	-1.48503900	-0.18315500

Table 7 Cartesian coordinates of second transition state of 2,3-dimethyl-2,3-pentanediol with one molecule of water in pinacol rearrangement by B3LYP/6-311^{+}G(d,p) method.

Atomic Type	Coordinate (Angstroms)		
	X	Y	Z
C	-1.27243300	-0.21488800	-0.55617100
C	-2.69521700	-0.81245900	-0.59802200
H	-3.26153100	-0.60897800	0.31438500
H	-3.24656100	-0.36790500	-1.43543600
H	-2.64629000	-1.89378400	-0.75273200
C	-1.31404200	1.34575700	-0.46098400
H	-0.28451700	1.70685900	-0.56771300
H	-1.84136900	1.65257700	-1.37568300
C	-0.94142800	-0.67323300	2.00114400
H	-0.18942900	-0.10508300	2.56421700
H	-1.89342100	-0.15472300	2.09650500
H	-1.02193700	-1.64689300	2.49669300
C	0.63235800	-1.68230400	0.29524000
H	1.09223500	-2.23065000	1.11649900
O	2.19428600	0.61446500	-0.16170900
H	3.15293700	0.51615500	0.15521400
O	-0.57515200	-0.53016200	-1.76808500
H	-1.12268100	-0.23533100	-2.51344500
H	2.24314400	0.72450200	-1.13764500
C	-0.49938100	-0.86999700	0.57571500
H	1.44995000	-0.50406900	0.05293200
H	0.70417100	-2.12850800	-0.69877100
C	-1.99755300	2.03051600	0.72561000
H	-1.48616600	1.85618500	1.67610800
H	-1.99332300	3.11275600	0.55748500
H	-3.04415700	1.72512500	0.83114200
O	4.79352000	0.30103000	-0.03947100
H	5.34098500	1.10332400	-0.02578600
H	5.27290700	-0.34457700	0.50495000

Table 8 Cartesian coordinates of second transition state of 2,3-dimethyl-2,3-pentanediol with one molecule of water in pinacol rearrangement by B3LYP/6-311^{+}G(d,p) method.

Atomic Type	Coordinate (Angstroms)		
	X	Y	Z
C	-1.41095100	0.10808000	-0.36341500
C	-1.38418800	-0.24904400	-1.67742500
H	-1.60293100	-1.26116700	-2.00313300
H	-1.34480200	0.51396900	-2.45134000
H	-0.02805700	-0.46125300	-1.59273600
C	-1.31450800	1.57638100	-0.00254500
H	-0.61505900	1.72201000	0.82470600
H	-0.90250800	2.11962200	-0.85694900
C	-1.90472300	-2.33024600	0.30334500
H	-2.01113600	-2.96066900	1.18583500
H	-2.83805600	-2.38470900	-0.26458900
H	-1.11813100	-2.76690300	-0.32043900
C	-1.48831700	-0.57281100	1.99840100
O	1.40002400	-0.76946100	-1.64465900
H	1.64228000	-0.99326000	-2.55671500
C	-1.58820300	-0.90753200	0.70186600
H	-1.27421300	0.43376600	2.33218700
H	-1.63040000	-1.31419800	2.77592000
H	2.07293200	-0.06447800	-1.17488100
O	2.86118700	0.79205000	-0.48200900
H	3.24499300	1.56493300	-0.91212000
H	3.53191100	0.44105400	0.15856000
H	5.28510600	-0.84450800	1.14215700
O	4.79665600	-0.01410700	1.17078600
H	4.91089800	0.33722700	2.06136200
C	-2.68868200	2.18086800	0.36414300
H	-2.97010600	1.95632800	1.39343600
H	-2.66339600	3.26605600	0.24800100
H	-3.47483500	1.79415000	-0.28842000

VITA

Mr. Tadtanu Shanyib was born on July 8, 1981 in Bangkok, Thailand. He received his Bachelor's degree of Applied Science in Chemistry from King Mongkut 's institute of technology North Bangkok in 2002. He has been a graduate student studying in the programe of Petrochemistry and Polymer Science at Chulalongkorn University and become a member of Supramolecular Chemistry Research Unit under the supervision of Associate Professor Dr. Vithaya Ruangpornvisuti. He finished his study in Master's degree of Science in 2006.